Bates College
SCARAB

Honors Theses | Capstone Projects

5-2018

Urbanization: Impact on Dissolved Oxygen and Sedimentation in the Hart Brook Watershed (Lewiston, Maine)

Hannah Rae Slattery
Bates College, hslatter@bates.edu

Follow this and additional works at: https://scarab.bates.edu/honorstheses

Recommended Citation
Slattery, Hannah Rae, "Urbanization: Impact on Dissolved Oxygen and Sedimentation in the Hart Brook Watershed (Lewiston, Maine)" (2018). *Honors Theses*. 243.
https://scarab.bates.edu/honorstheses/243

This Open Access is brought to you for free and open access by the Capstone Projects at SCARAB. It has been accepted for inclusion in Honors Theses by an authorized administrator of SCARAB. For more information, please contact batesscarab@bates.edu.

Urbanization: Impact on Sedimentation and Dissolved Oxygen in the Hart Brook Watershed (Lewiston, Maine)

Bates College Geology Honors Thesis

Presented to

The Faculty of the Department of Geology, Bates College

In partial fulfillment of the requirements for the

Degree of Bachelor of Arts

By

Hannah Rae Slattery

Lewiston, Maine

March 28, 2018

Acknowledgements

Thank you to all of the Bates College Geology Department: Beverly Johnson, Philip Dostie, Dykstra Eusden, Mike Retelle, Genevieve Robert, Alice Doughty, Marita Bryant, and Raj Saha. Thank you to CES Inc. and David Brooks for the invaluable internship experience and providing me with a springboard for this entire project. Additional thanks to Justin Early of Lewiston Public Works, Holly Ewing of the Bates College Department of Environmental Studies, and Ali Ahktar of the Bates College Religious Studies Department for their efforts.

I wish to extend my deepest gratitude and appreciation to my advisor Dr. Beverly Johnson. Without her undying support and guidance, I would not have completed this project and surely would not have experienced such growth. You are a role model to me, and I strive someday to be half as accomplished, confident, and intelligent. Bev is not only a mentor, but a friend, who shares a passion for meaningful, progressive work. Thank you endlessly, Bev.

Another absolutely integral, "north star" in this endeavor has been Phil Dostie. My lab and field work would never have been possible without your mentorship. Your knowledge of lab instrumentation, technology, and chemistry do not cease to amaze me on a daily basis, and, lastly, your company in the Geochemistry Lab always brightens my spirits.

I thank my mom, dad, and sister from the bottom of my heart. Family is the most important aspect of my life, and they have supported me from day one. I will keep working hard to make you proud.

My friends, peers, and classmates challenge, support, and inspire me. The Bates classroom has broadened my worldview and strengthened my values, and that is a reflection of the people who have gone through these experiences with me. In particular, I owe thanks to all Class of 2018 Geology majors.

Table of Contents

Table of Figures

Table of Tables

Abstract

As cities across the United States have urbanized, the amount of impervious surface (pavements, rooftops, cement, etc.) has risen steeply. Increases in imperviousness impact natural hydrologic processes in a watershed and can lead to a decrease in water quality (high sediment loads and low dissolved oxygen levels). In Lewiston, Maine, the Hart Brook watershed has 22% impervious surface cover (ISC) and is classified as an urban impaired watershed due to dissolved oxygen levels below 75% saturation and excessive nutrient loads during the peak of summer. Wastewater infrastructure has been surveyed and repaired in some locations, but very limited research has addressed sedimentation patterns. The purpose of this study is to evaluate the timing and extent of urbanization and its impact on sediment dynamics and water quality. Satellite images were analyzed using data from the National Land Cover Dataset to re-estimate total impervious surface cover within the Hart Brook watershed at 32.87%. A separate analysis of historical imagery was performed to estimate change in ISC over time within the watershed and found a 400% increase between 1953 and 1998. Additionally, a 150 cm sediment core was collected from a central floodplain and analyzed for grain size, %C, magnetic susceptibility, and lead concentrations. A geochemical age model using [Pb] and ^{14}C was used to constrain sedimentation rate over time. Three predominant theories are proposed to explain sedimentation rates in the watershed. A modern sedimentation model, based on normalized lead data and a ^{14}C date of 1950+ at 74cm, showed a rapid, minimum sedimentation rate of 2.24 (cm/yr) from 1923 to 1972 and a rate of 0.85 (cm/yr) from 1972 to 2017. A Holocene sedimentation model, based on raw lead data and the nature of the sediments, implied a sedimentation rate of 0.48 cm/yr between 1923 and 1972, and 0.85 cm/yr between 1972 and 2017. Finally, a historical model showed a sedimentation rate of 0.48 cm/yr between 1923 and 1972, and 0.85 cm/yr between 1972 and 2017, but was also extrapolated to the bottom of the 150cm core or the year 1781 using an average of the two rates, 6.4cm/yr.

1. Introduction

1.1 Overview

The past century has seen unprecedented rates of urbanization globally, and, as a consequence, amounts of constructed impervious surfaces have risen steeply. The sudden increase in impervious surface has impacted and impaired natural hydrologic processes, of which the most significant may be an increase in runoff to base flow proportions. Lewiston, Maine is no exception. In the local Hart Brook watershed, increased percent impervious surface cover (ISC) likely correlates to an acceleration in sedimentation rate and a decline in water quality. This study will use remote sensing techniques to estimate total impervious surface cover of the watershed at 3 times steps, 1953, 1998, and 2017. Results will then be compared to sedimentation rates on the floodplain using a lead age model and to recent dissolved oxygen concentration data. This is a local study, but the implications are much larger. Development recommendations for percent impervious surface cover can prevent water quality degradation in growing cities across the globe and help subvert public health crises. This chapter will, first, provide a brief history of the Hart Brook watershed, then, a discussion of the body of literature that already exists on this topic, and, finally, a background of the case study.

1.2 History of Hart Brook

The state of water quality in Lewiston, Maine has been a prominent issue since the early 1940s. Most concern was focused on the pollution of the Androscoggin River by local paper mills. A monitoring report conducted in 1940 recorded there was no dissolved oxygen in the Androscoggin River (Chase, 1960). For reference, Article 4-A: of the Maine Water Classification Program holds a standard of 75% saturation for dissolved oxygen in Class B waters. Remediation efforts began in the mid-1940s and Walter Lawrence, a Bates Chemistry Professor, was appointed the River Master of the Androscoggin River by the Maine Supreme Court in 1947. His duties consisted of setting limits on paper pulp discharge into the Androscoggin River, suggesting remediation practices (including dumping vast quantities of sodium nitrate into the river and building detention tanks for paper waste), and keeping diligent records of the state of water quality.

No such records exist for the Hart Brook, and the topic of raw sewage dumping into both the Androscoggin and Hart Brook has been dwarfed by the paper mill industry. Despite the waste and pollution causing a comparable amounts of public disturbance in the local area, only sporadic press reports exist as a historical lens into the conditions of Hart Brook during the 1940s and 50s. On February 26, 1959 the following quote was published in the Lewiston Evening Journal on the matter of whether or not to construct a sewer system for the Hart Brook watershed:

"This open sewer collection system, draining 1,200 acres of land bordered by East Ave., Pleasant St., Lisbon Road at North American Philips Corp., and the Androscoggin River, has existed for years although condemned by the State in 1941. It did not become a menace until the last 10 years, when South Lewiston exploded in a tremendous build-up of housing developments, commercial developments and the Industrial Park, that overwhelmed the system and created the monstrosity that it is today. Twelve-inch rats, running in the streets were flushed like quail when the surveyors went through the areas. The odor is unbearable year around except in sub-zero temperatures. Bugs and insects in astonishing numbers grow two to three times their normal size from the lush vegetation caused by human waste. The dread staphylococcus germ and typhoid are the disease that constantly menace the people as Dr. Wiseman pointed out."
- (Lewiston Evening Journal, 1959 and Lawrance, 1959)

Truly, this account evokes images straight out of a science fiction film, and it is not the only anecdote that used such graphic language and disturbing descriptions of the Hart Brook in the late 1950s. Looking past the outright disgust, though, a couple of key concepts relevant to this particular study are captured in the above quote. First, the role of urbanization is explicitly referenced as a cause of the contamination of the watershed (Lawrance, 1959). Although sanitation issues had been present beforehand, the rapid development and addition of impervious surfaces accelerated and proliferated disease and extremely poor water quality (Lawrance, 1959). Raw sewage was easily swept into the river, without any opportunity to infiltrate into the soil and undergo natural purification.

In the 1950s, the threat of disease and illness loomed ever-present in Hart Brook, and locals were met daily with public health hazards. Residents of the watershed were contracting staphylococcus germ and typhoid, bacteria from fecal matter (Lawrance, 1959). The exposure

may have happened through drinking water or simply close proximity and exposure from impervious surface runoff. Eventually, after much debate of fiscal costs and health benefits, the sewer plan was approved and construction was completed in 1963 (Chase, 1960).

Water quality issues were not as frequent a conversation in Lewiston again until it was discovered by the Maine Department of Environmental Protection (MDEP) that the stream was not meeting water quality standards for bacteria and dissolved oxygen in 1998. A rejuvenated interest in the watershed lead to further monitoring in 2003 and 2005. In 2004, Hart Brook was listed as an urban impaired stream for falling below the state water quality requirements for the minimum water quality classification. In 2007, a Hart Brook Watershed Action Plan was developed by Woodard and Curran, a local environmental consulting firm. This project was funding by the City of Lewiston and included reforms to street sweeping, planting of rain gardens, educational and volunteer monitoring programs, and more (Woodard and Curran, 2007). A limited number of these reforms have been implemented, such as rain gardens and street sweeping.

Where do these issues fit in the larger picture of research already published? Are these isolated problems or evidence of well-established trends? The following section will situate the Hart Brook urbanization, sedimentation, and water quality issues into a larger bed of literature.

1.3 Review of Literature

1.3.1 Impervious Surface Area (ISA) and Declining Water Quality:

The discussion surrounding the impact of impervious surface area on water quality has often been framed using degradation thresholds. The most widely known and commonly used ISA thresholds for any given watershed are as follows: 1-10% = stressed, 10-25% = impacted, above 25% = degraded (Arnold and Gibbons, 1996).

There is great variability in how different biotic and abiotic factors respond to impervious surface cover. Fish and benthic invertebrates have much lower thresholds, around 4-15%, than many abiotic factors like metals, nutrients, and base flow, all between 45-50%. Biotic factors typically have lower degradation thresholds than abiotic factors. Figure 1.3.1 is a summary of degradation thresholds for a number of important variables (Brabec et al. 2002).

Parameter type	Impact Measurement	Percentage Impervious Threshold for Degradation	Study
Biotic	Benthic invertebrates	< 10 humans per hectare	Jones and Clark (1987)
		8	Horner et al. (1997)
		15	Klein (1979)
	Fish diversity	10 urbanized	Limberg and Schmidt (1990)
		12	Klein (1979)
		8	Miltner (1997)
		3.6	Booth and Jackson (1994)
		10	Wang et al. (forthcoming)
	IBI	8 urban land use	Yoder et al. (n.d.)
	Macroinvertebrate diversity	8 to 15	Shaver et al. (1994)
		8	Miltner (1997)
	Species diversity	10 to 15	Booth and Reinelt (1993)
Abiotic and biotic	IBI, habitat quality	10 to 20 urban land use	Wang et al. (1997)
	Mean event water-level fluctuation/ indicator species	10 TIA, 14 EIA	Taylor (1993)
	Variation of water depth and indicator species	15 to 21	Chin (1996)
Abiotic—physical	Temperature for cold-water biota	12	Galli (1990)
	Base flow	45	Klein (1979)
	Stream flow	> 21	Horner et al. (1997)
		Not defined	Krug and Goddard (1986)
	Peak flows	4.6	Booth and Jackson (1994)
	Channel enlargement and streambank erosion	Not given	Hammer (1972)
		34 urbanization	MacRae (1997)
		8 to 10	Booth and Reinelt (1993)
		30	May et al. (1997)
		10	Booth and Jackson (1994)
	Habitat assessment	4 to 9 impervious surface and 30 to 50 forest	Hicks and Larson (1997)
	Large woody debris	9	Horner et al. (1997)
	Sediment	20	Wydzga (1997)
		50	Horner et al. (1997)
		Not defined	Krug and Goddard (1986)
		43	Griffin et al. (1980)
		45	May et al. (1997)
Abiotic—chemical	Nutrients	42	Griffin et al. (1980)
	Phosphorous	45	May et al. (1997)
	Threshold of eutrophication based on TSS and TP	30	Todd et al. (1989)
	Chemical water quality	45	May et al. (1997)
	Oxygen	10	May et al. (1997)
		7.5 urbanized	Limburg and Schmidt (1990)
		43	Griffin (1980)
	Metals	50	Horner et al. (1997)
	Zinc	40	Horner et al. (1997)

NOTE: IBI = Index of Biotic Integrity; TIA = total impervious area; EIA = effective impervious area; TSS = total suspended solids; TP = total phosphorus.

Figure 1.3.1: Biotic and Abiotic Thresholds for ISA Water Quality Degradation (Brabec et al., 2002)

Brabec et al., (2002) addresses the need to limit impervious surface cover, but also to protect and keep natural water filtration processes intact. Pervious surfaces like gravel driveways and bare soil essentially function like impervious surfaces. Infiltration is ineffective, in part due to soil compaction. Mature forests are highly absorbent. Protecting mature environments paired with impervious surface regulations are needed to ensure healthy ecosystem functioning.

Brabec et al. (2002) problematizes the use of a universal threshold for impervious surface cover, beyond which significant degradation will occur. The threshold would be highly variable depending upon land use within a single watershed. A high density city center would not have the same impervious surface threshold as an agricultural area. Essentially this means that throughout a single watershed there can be major variations in the intensity of impervious

surface cover that can generate different magnitudes of degradation. Relationships exist between land-use and ISA. Land designated as industrial and commercial almost always has a very high % impervious surface cover, while large residential lots typically have very low % impervious surface cover (Arnold and Gibbons, 1996). Typically, a more nuanced spatial analysis of the watershed can avoid issues of generalization and isolate areas of degradation more easily and accurately.

Impervious surface cover itself is not what causes poor water quality, but it is the vehicle that transports pollutants and excessive amounts of runoff into a stream or river. Pavements and rooftops collect and consolidate precipitation to generate these large volumes of high velocity runoff. Most roofs have gutter systems that direct precipitation either into yards/lawns or driveways (Woodard, 2007). Gutters that release onto driveways are especially destructive because they do not offer any opportunity for infiltration. All of the water becomes runoff. Lawn precipitation disposal presents a separate set of issues. The water may infiltrate into the soil, but it also may collect nitrogen and other nutrients from residential fertilization. If lawn soils receive a lot of precipitation and are relatively newer construction, they may also have less consolidated soils that are susceptible to erosion. High concentrations of nitrogen and organic material running directly into a stream will likely cause a decrease in dissolved oxygen concentrations as well as an increase in whatever chemicals, salt, bacteria and waste were left on the roadways.

The process of lowering dissolved oxygen levels requires some digesting, both literally and figuratively. The addition of nutrient rich runoff into a stream (Pedersen and Calvert, 1990) is likely to stimulate high levels of biologic decomposition (Wu, 2002). Decomposers respire while breaking down organic material, so the dissolved oxygen in the water is lowered (Diaz and Rosenbug, 2008). Respiration outpaces photosynthetic processes when there are large nutrient inputs, so the dissolved oxygen levels have the potential to become dangerously low to sustain ecosystem functioning.

If levels of imperviousness are high enough, runoff can also carry sediments in addition to a dissolved organic load. The input of sediment and soil into the stream causes increased turbidity in the water. The turbidity, or cloudiness, represses vital, oxygen-producing, photosynthetic processes, as there is no longer a consistent source of sunlight (Parkhill and

Gulliver, 2002). The sunlight is blocked and deflected by the suspended sediment load rather than absorbed by photosynthetic organisms. As the availability of sunlight declines, fewer photosynthetic organisms can survive in the stream.

In addition to the hydrologic relationships already discussed, (Klein, 1979) found that as % impervious surface cover increases: base flow decreases (see figure 1.3.2 A), biodiversity declines (see figure 1.3.2 B), stormwater runoff increases, the frequency and severity of flooding increases, channel erosion accelerates, the stream bed composition is altered, the natural stream temperature regimen is altered, toxic substances (i.e. heavy metals pesticides, oil road salt) increase, and nutrient, especially nitrogen (Wahl et al, 1997), levels increase.

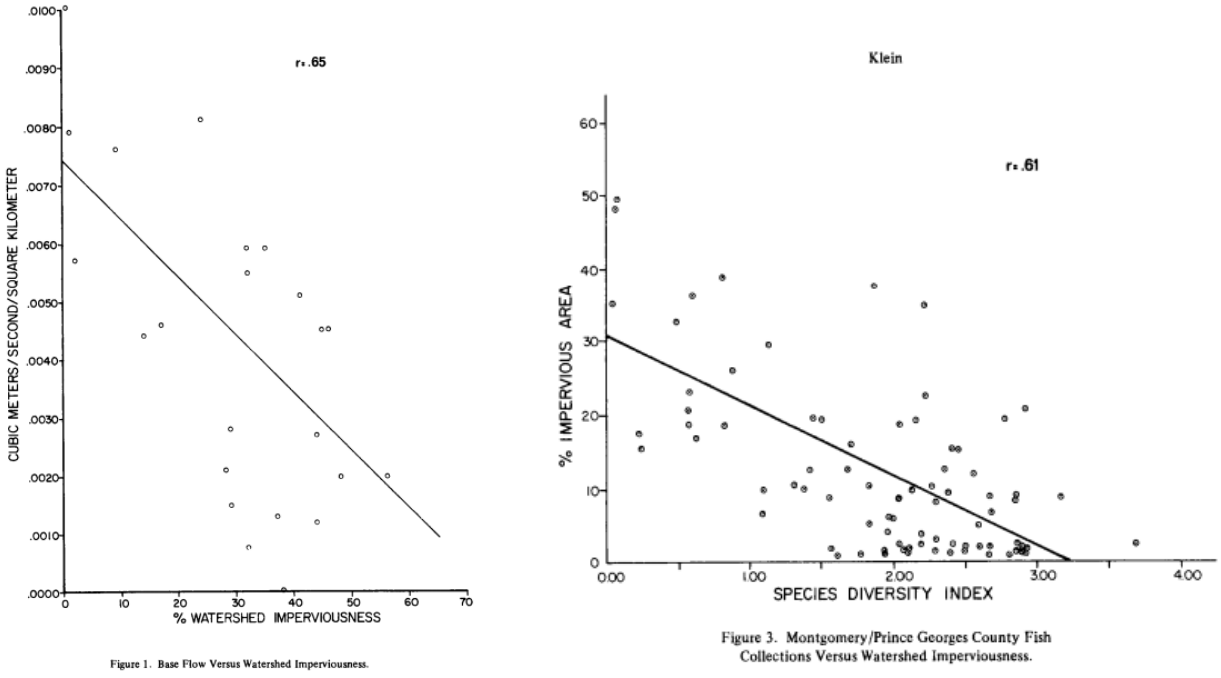

Figure 1.3.2: (A) shows the inversely proportional relationship between ISA and base flow (B) shows the inversely proportional relationship between ISA and species diversity (Klein, 1979)

1.3.1a ISA and Sediment Dynamics

A number of previous studies have quantified and investigated the relationship between urbanization and sedimentation (Krug and Goddard, 1986) (Freeman and Schorr, 2004) (Walters et al., 2003) (Booth, 1990) (Ormerod, 1998). Despite variations in location, water-body size, and type, each source found a positive correlation between imperviousness and sedimentation. Krug and Goddard (1986) found a stream bed lowered or eroded away by nearly two feet in the span of six years. Booth (1990) quantified that streambank erosion and sediment loads increase when impervious surfaces are at higher elevation within a watershed. Walters et al. (2003) observed a trend of increasingly fine-grained stream beds and turbid waters as urban development expanded in a watershed.

Turbidity and fine-grained sediments are two major detriments to ecological health in urban streams. Benthic-invertebrates, particularly pollution-sensitive insects, experienced declines in small-midsized streams due to increases in sedimentation caused by urbanization (Freeman and Schorr, 2004). Additionally salmonid and other endemic spawning fish species have seen decline as fine sediments disrupt and inhibit natural spawning processes (Walters et al., 2003).

All of the above-listed studies focus on sedimentation patterns within a narrow window of time, on the scale of days to years, but lack a broader view of sedimentation dynamics. Caesium-137 studies like Ormerod (1998), and lead age-dating can offer a more expansive view decades, centuries, and, in some cases, even millennia long. Cs-137, an artificial radionuclide, was generated by atmospheric nuclear testing between 1952 and 1980 (Cambray et al., 1989). Concentrations of Cs-137 in soil, like lead, are now measured for variations related to anthropogenic activity to date the sediment. A benefit of using Cs-137 or lead dating is that a larger expanse of time can be represented than by water sampling, geomorphologic measurements, or any other acute or one-time techniques. The downside is that long-term dating may not achieve a high level of nuance, for example, changes in seasonal runoff and precipitation or storm events, which acute sampling can detect.

In addition to a narrow time-scale of sedimentation, much of the current literature does not adequately constrain processes related to urbanization. Knowledge of when and how much ISA was added to the watershed informs discussions of sedimentation. This likely relates to the fact that acute sampling practices would not necessitate knowledge of urban development over time, but rather the total amount of ISA at the given moment the sample or measurement was taken. This study will attempt to serve as a hybrid between long-term (lead sediment dating and historic aerial imagery analysis) and acute (water quality sampling of D.O. and Temperature) techniques to provide a comprehensive analysis of the relationship between sedimentation and urbanization over time.

1.3.1b Calculating Impervious Surface Area (ISA):

A major component of impervious surface studies is the spatial calculation of ISA within a watershed. This step is often made invisible by the larger findings to do with ecological health, thresholds, and even stream morphology, but using the most sophisticated technologies and methods can significantly improve the accuracy of ISA calculations. Before aerial photography, estimates were often done by field surveying and mapping. Aerial imaging took off in the 1970s and 1980s, but there were significant obstacles related to image resolution and image processing technology (Weng, 2012). Publishing and authorship of remote sensing literature increased the most drastically entering the 21st century and continues today (Weng, 2012).

Weng, (2012) delves more deeply into the technical aspects of remote sensing. Spatial resolution is "a function of sensor altitude detector size, focal size and system configuration," (Jensen, 2005), and "it defines the level of spatial detail in an image," (Weng, 2012). Spatial resolution allows you to make out specific objects within an image. In colloquial terms, it is the level or lack of blurriness. If an image is blurry and you cannot describe its details, it likely has poor resolution. It is difficult to construct historical impervious surface cover records for this very reason. The resolution is often too low to identify impervious surfaces.

More recently, high resolution satellite imagery has quelled resolution worries, but added a new set of obstacles. Shadowing, cloud cover, and slight differences in wavelength (pixel color) can cause classification errors, but the spatial analysis techniques implemented in this study have taken care to select methods that address these concerns.

1.4 History of Lead Deposition and Dating

Lead concentrations and fluxes have varied long before anthropogenic activities like agriculture, smelting, mining, and transportation, but never to the same magnitude as human-induced changes. One of the longest chronologic sediment-based records of lead deposition found that climatic changes caused enhanced lead levels in approximately 10,590 14C yr BP (the Younger Dryas) and in 14C yr BP (Shotyk et al., 1998). Multiple other studies address the variability of lead before industrial activity using ice cores. (Boutron et al., 1995 and Renberg et al., 2000). These studies reinforce that lead is, at its essence, a naturally occurring element that is influenced by natural processes including volcanism and erosion. The first marked anthropogenic induced increase in lead deposition took place beginning in 3000 14C yr BP, catalyzed by deforestation and agricultural clearing (Shotyk et al., 1998). In 0 AD, the peak in lead production during the Roman period contributed to a pronounced increase. Roman lead production is

more diagnostic in soils of Northern Europe than the United States, but is a major change, nonetheless, and was one of the first instances of trade, construction, and direct use of lead in human society (Renberg et al., 2000). The medieval period, particularly from 1000–1200, showed another significant period of lead deposition in European soils due to mining and additional metal production (Renberg et al., 2000).

Beginning in 1750 in Europe and 1850 in the United States, the Western world experienced industrializations that revolutionized the use of lead in human society. Smelting and mining occurred at prolific rates and, finally, in the early 1920s (1923) the burning of alkyl-leaded petrol in automobile engines catalyzed the most pronounced change in global lead records the world had ever seen. Concentrations are estimated to have increased from 10 pg/g in the second half of the 1700s and the early 1800s to approximately 200 pg/g or more at the peak of leaded gasoline consumption in the United States during the mid-1960s, a 20-fold increase (Renberg et al., 2000). According to a different study (Callender, 2004) the mean annual atmospheric concentration of lead in the atmosphere nearly tripled in value in the 1950s. The impact of burning leaded gasoline caused a ubiquitous increase in lead concentrations, from Maine to Switzerland and beyond, and are observable in everything including soils, pollens, drinking water, tree rings, and human health. Concentrations began to decline sharply after the banning of leaded gasoline in the United States in 1972 as part of the Clean Air Act (Callender, 2004).

Where does the Hart Brook and the HB-3 core tie into all of this? Judging by the sequence of lead deposition described above, the core should contain a record of burning leaded gasoline, and the shallowest modern peak should correspond well to the banning of leaded gasoline in 1972. It is also expected that there will be a leveling off or return to baseline values further down core, at which the depth will correspond to the onset of the burning of leaded gasoline or approximately 1923.

In terms of overall sedimentation rates, a study by (Pizzuto et al., 2016) conducted significant research and review of existing sedimentation rates on floodplains with a wide breadth of spatial variability. 107 floodplain cores were analyzed using Mercury-dating and combined with existing data to find median sedimentation rates of: 3.8 cm/100 years, 1.37 cm/100 years, 0.4 cm/100 years, 0.1 cm/100 years. These values will be used in later sections of this study to make comparisons between sedimentation rates found in previous literature and sedimentation rates found in the Hart Brook watershed.

1.5 Hart Brook Case Study

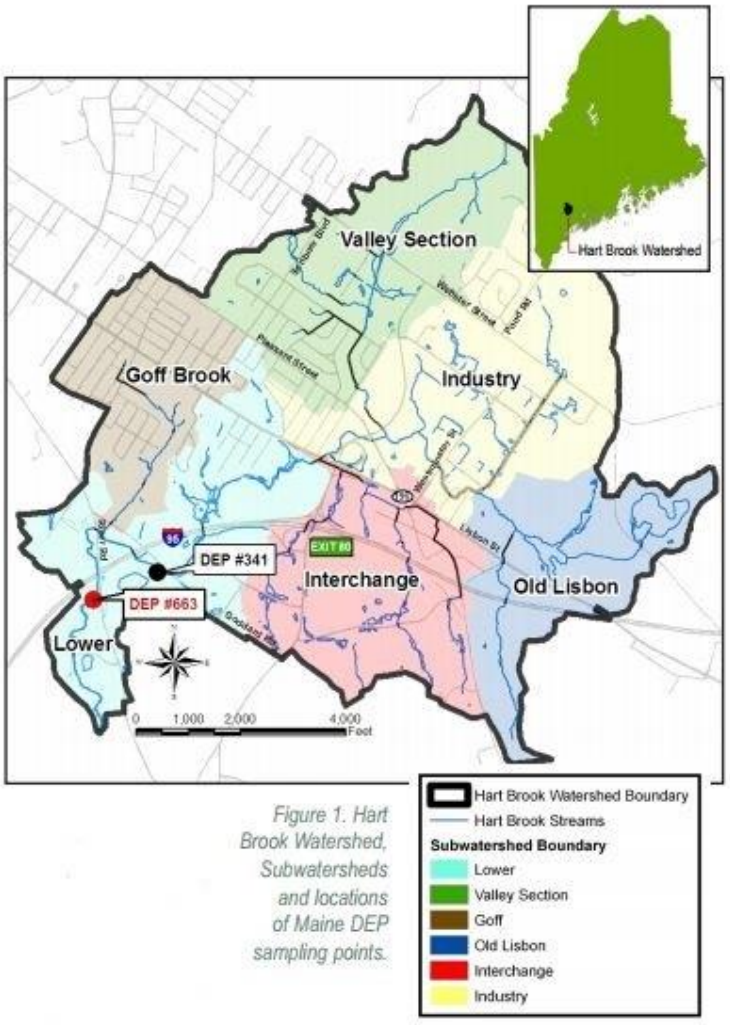

Figure 1. Hart Brook Watershed, Subwatersheds and locations of Maine DEP sampling points.

Figure 1.4.1: Hart Brook Watershed (MDEP TMDL Assessment Summary, 2013)

Hart Brook is a stream located in the city of Lewiston, Androscoggin County, ME. The entire stream is 3.7 miles long and has a 2100 acre watershed. It is further broken into 6 sub-watersheds (Fig. 1.4.1) for management purposes by the Maine DEP. The Maine DEP determined the watershed has 22% impervious surface cover (MDEP). These calculations were performed using 1998 aerial imagery, but are now outdated. Additionally, the methods of the DEP calculations were never publicized. Figure 1.4.2 shows the distribution of impervious surfaces throughout the watershed. The eastern central section of the watershed is home to an industrial park and the most concentrated area of impervious surface cover.

In 2004, Hart Brook was declared a Class B urban impaired stream for falling below three state water quality requirements, stipulated in the Clean Water Act of 1972 (MDEP). The criteria included two regulations for dissolved oxygen and one for *Escherichia coli* bacteria. Dissolved oxygen may not fall below 7 parts per million or 75% of saturation, whichever is lowest (MDEP). For *Escherichia coli* bacteria, between May 15th and September 30th, numbers may not exceed a geometric mean of 64 per 100 milliliters or an instantaneous level of 236 per 100 milliliters (MDEP).

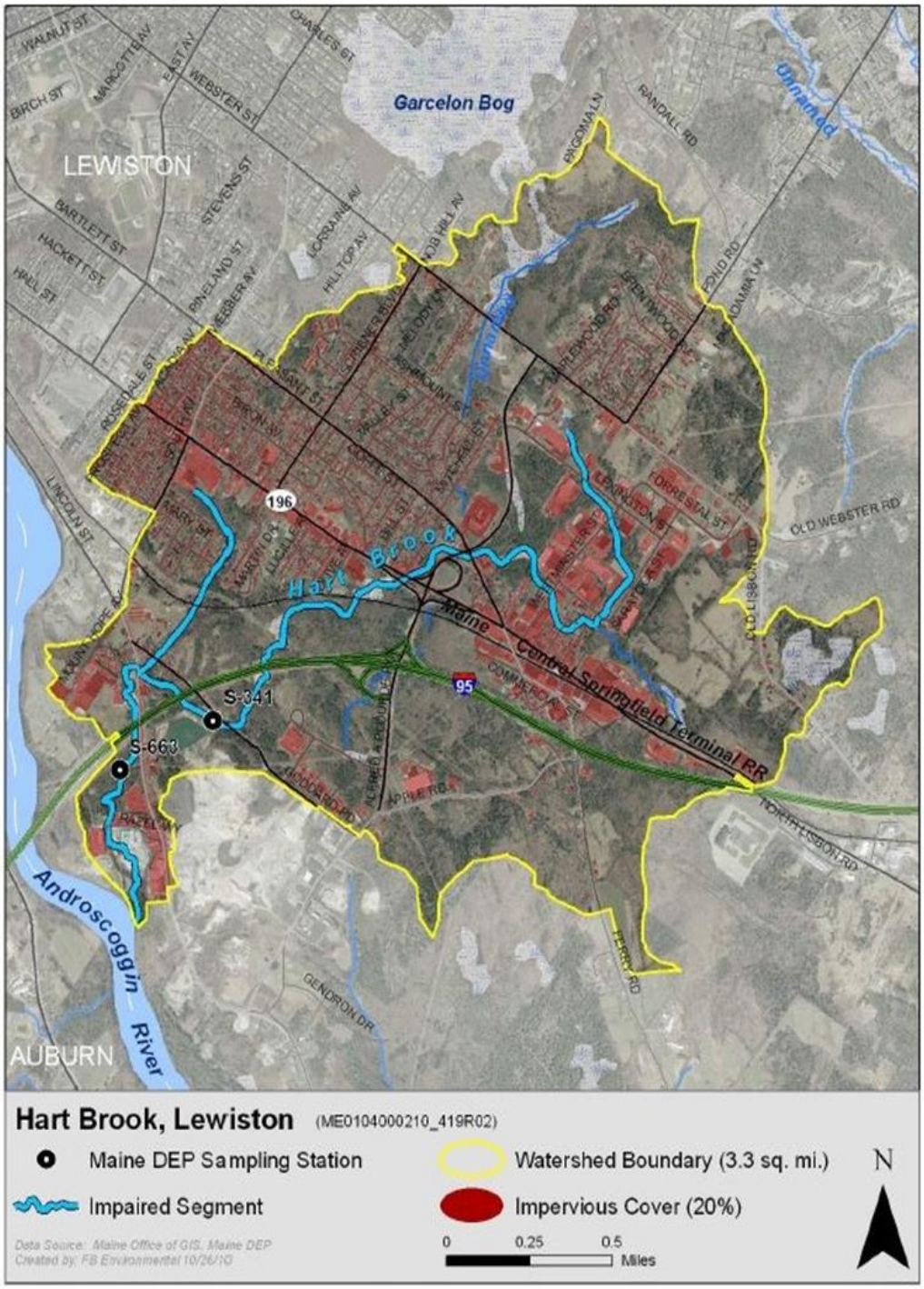

Figure 1.4.2: (MDEP TMDL Assessment Summary, 2013) Map of Hart Brook Watershed Impervious Cover

In 2013, 2014, and 2015 Total Maximum Daily Load (TMDL) assessments were performed by the MDEP to monitor the condition and progress of Hart Brook. The dissolved oxygen results from the three MDEP TMDL reports in 2013, 2014, and 2015 (shown respectively in figure 1.4.4) have clear geographic trends and areas of concern. HB2 and HB4 have at least one impaired measurement from each year of monitoring. In 2013, HB4 had all measurements below the 75% saturation standard, while HB2 had four out of five impaired measurements. Finally, in 2015, HB2 had only one measurement below the standard, but HB4 had two out of three below the standard. After the first TMDL assessment in 2013, measurements were frequently taken at only some of the sites during each visit and show a much more random schedule of collection. While this may better highlight variations in dissolved oxygen concentrations at certain sites and times, it may bias results by ommitting water quality shifts that occur in response to short term weather patterns, especially precipitation events. A more frequent and standardized method of data collection would allow for a better understanding of dissolved oxygen impairment in Hart Brook.

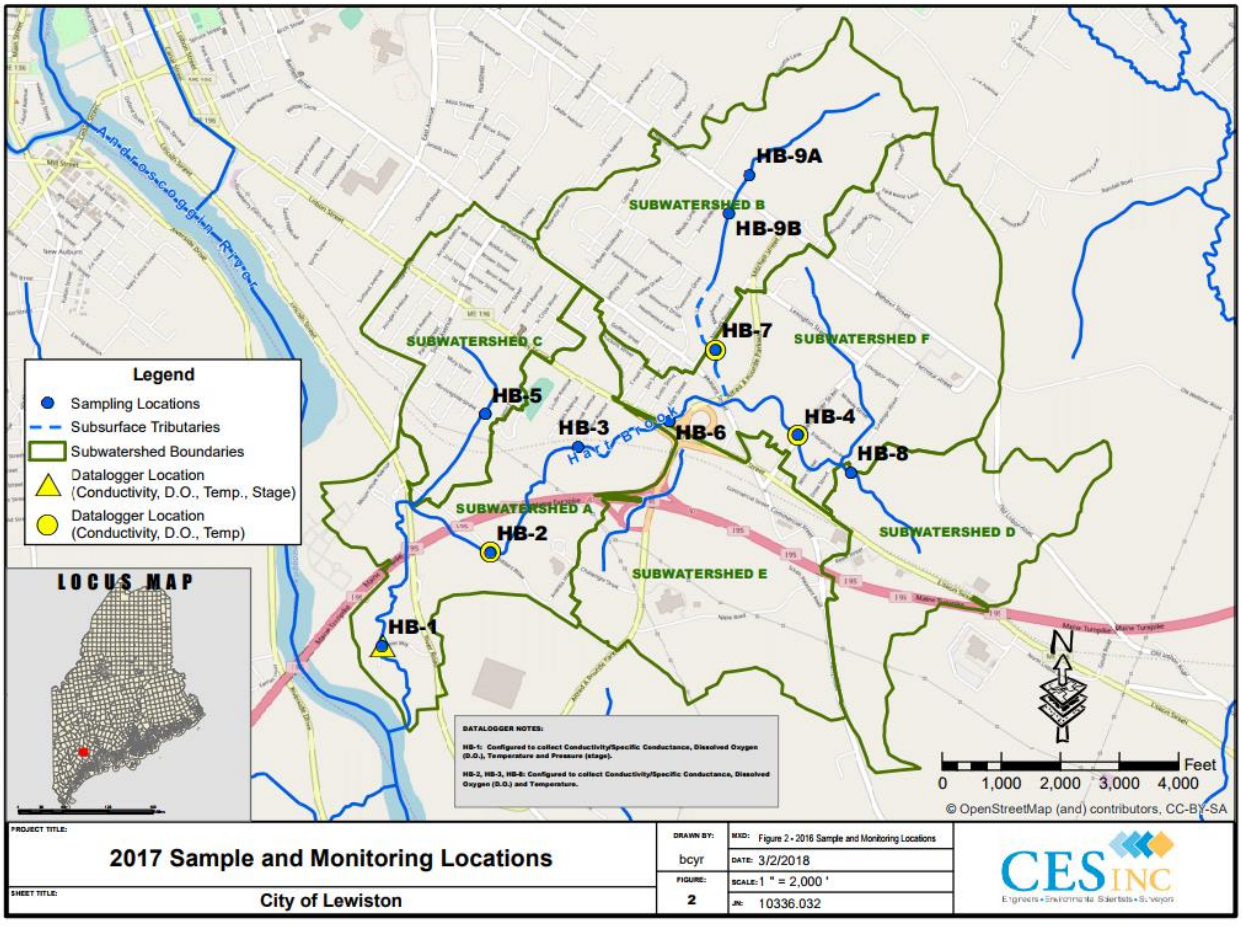

Figure 1.4.3: Hart Brook Water Quality Sampling Sites

Figure 5-4-4: Graph of dissolved oxygen saturation

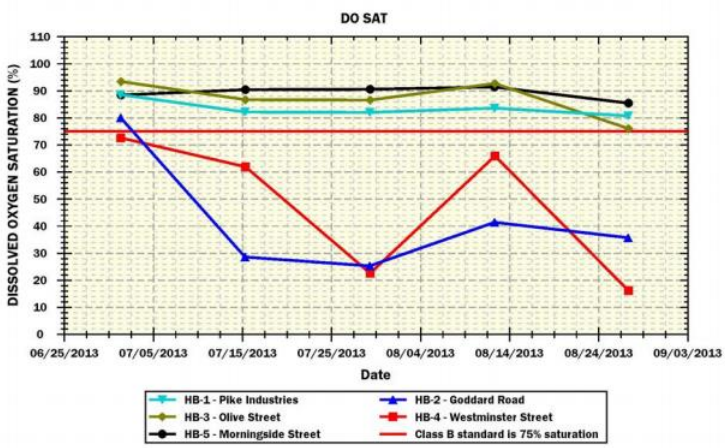

Figure 5-4-4: Graph of dissolved oxygen saturation for the main stem sites.

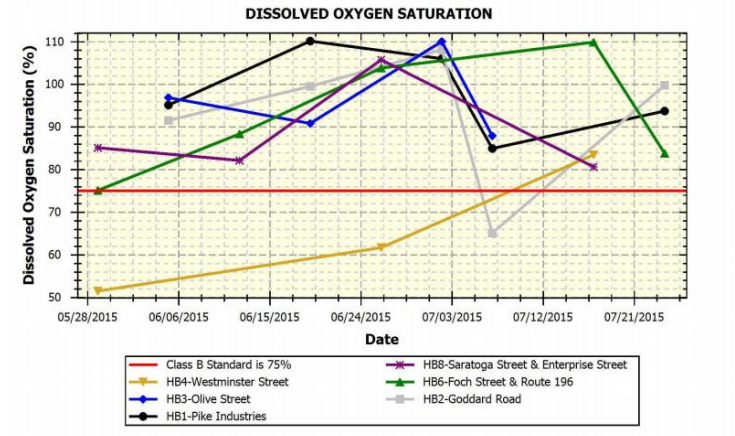

Figure 5-4-4: Graph of dissolved oxygen saturation for the main stem sites.

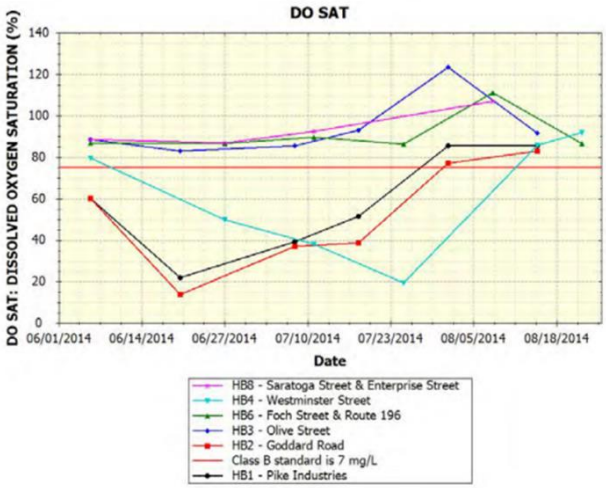

Figure 1.4.4: (MDEP 2013, 2014, and 2015) Hart Brook City of Lewiston Data Reports

It is difficult to see the seasonal nuances in Hart Brook and at these sites specifically with such limited and inconsistent data collection. This study will attempt to provide a more consitent and longer time span of data for both water quality, specifically dissolved oxygen, and sedimentation rate on the flood plain. A sedimentation study has never been performed at this study location before.

1.6 Summary of Introduction

Although general trends and thresholds exist for ISA, it is essential to remember that each individual watershed has its own individual characteristics, and even overall estimates of impervious surface cover cannot predict what processes will take place and to what extent. The focus of the Hart Brook case study will be placed on sedimentation rate analysis and dissolved oxygen data assimilation. This is the first ever known study to investigate and determine a sedimentation rate using various core analyses (lead and ^{14}C dating) and to compare that rate to increasing impervious surface development using spatial imagery analysis. This study fills a much needed gap in process and geomorphologic based assessment of the effects of increasing ISA. Remediation efforts will not be covered in this paper though many exist and progressive efforts have taken place in select locations across the United States.

2. Methods

Introduction to Methods:

The methods of this study can be split into three broad categories: spatial analyses, core analyses, and water quality monitoring.

The spatial analyses will serve three main purposes. First, it will utilize a new technology and dataset to re-estimate impervious surface area (ISA) in the Hart Brook Watershed, as the historical Woodard and Curran (2007) calculation was found to be outdated and inaccurate. Second, it will calculate change in ISA from 1953 to 2017 to track development trends over time, which will later be compared to sedimentation trends. Third, it will repeat the original Woodard and Curran (W&C) calculation, as no methods were published.

The core analyses contain subsections 2.3-2.7, including coring and subsampling, lead analysis and dating model, percent carbon content, magnetic susceptibility, and grain size analysis. The lead analysis and dating model will later be used to place temporal constraints on sedimentation. Carbon content will be used to normalize lead data, as lead sorbs more efficiently to carbon than inorganic substrate. All other analyses will supplement understanding the stratigraphy and hydrologic properties of strata at various depths within the core, including soils, clay, sand and gravel.

Finally, water quality monitoring, the last subsection, will describe field methods related to periodically measuring various water quality parameters. The most important measurements to this study will become temperature and dissolved oxygen because of their relationship to impervious surface cover and sedimentation (or organic deposition).

At large, the methods and analyses herein hope to answer the following question:

How has urbanization impacted sediment dynamics, and, subsequently, the water quality within the Hart Brook Watershed?

2.1 Impervious Surface Area Calculation

2.1.1 NLCD Method

The aerial imagery analyses performed in this this section intend to resolve important methodological discrepancies related to the total amount of ISA within the Hart Brook Watershed.

Total impervious surface cover in the Hart Brook watershed was calculated in ArcGIS, using a series of tools and analyses. Datasets were taken from the 2011 National Land Cover Dataset (NLCD) and uploaded into GIS. Each dataset had the following layers (shown in figure 2.1.1): Developed (Open Space), Developed (Low Intensity), Developed (Medium Intensity), Developed (High Intensity), and Barren Land (Rock/Sand/Clay). Additionally, each land type had a specific value range for % Impervious Surface Area. This range was averaged to produce a single value for % ISA by land type (also shown in figure 2.1.1).

		% ISA By Land Type
Developed		
21	**Developed, Open Space** - areas with a mixture of some constructed materials, but mostly vegetation in the form of lawn grasses. Impervious surfaces account for less than 20% of total cover. These areas most commonly include large-lot single-family housing units, parks, golf courses, and vegetation planted in developed settings for recreation, erosion control, or aesthetic purposes.	10 %
22	**Developed, Low Intensity** - areas with a mixture of constructed materials and vegetation. Impervious surfaces account for 20% to 49% percent of total cover. These areas most commonly include single-family housing units.	35 %
23	**Developed, Medium Intensity** - areas with a mixture of constructed materials and vegetation. Impervious surfaces account for 50% to 79% of the total cover. These areas most commonly include single-family housing units.	65 %
24	**Developed High Intensity** -highly developed areas where people reside or work in high numbers. Examples include apartment complexes, row houses and commercial/industrial. Impervious surfaces account for 80% to 100% of the total cover.	90 %
Barren		
31	**Barren Land (Rock/Sand/Clay)** - areas of bedrock, desert pavement, scarps, talus, slides, volcanic material, glacial debris, sand dunes, strip mines, gravel pits and other accumulations of earthen material. Generally, vegetation accounts for less than 15% of total cover.	100 %

Figure 2.1.1: (NLCD) Land Type and Average % Impervious Surface by Land Type

The NLCD data was provided as raster data, so it was converted to a polygon feature before calculating total area. The extract by mask tool was used so that the polygon output feature would be of the correct data type (vector) and the correct shape (the Hart Brook Watershed). To do this an outline feature of the watershed was used as the mask.

To find the area of a given land type within the watershed, the attribute table was opened and sorted by land type. All of the features from one land type were selected and the statistics function was used to generate the total area of that land type. Then, the specific % ISA of the

land type (figure 2.1.1) was multiplied by the value for total area for the land type, to solve for area of impervious area within one land type. These calculations were repeated for each land type and then added together to solve for total impervious surface area in the Hart Brook Watershed. Finally, total area of Hart Brook was divided by the total ISA of Hart Brook and multiplied by 100 to solve for % impervious surface cover of Hart Brook. Summary calculations:

Area by Land Type (m^2) * % ISA by Land Type = ISA by Land Type (m^2)

[Total watershed area (m^2) / Sum of IS for all Land Types (m^2)] *100 = % Total watershed ISA

2.1.2 Tracing Method

A second method was chosen to evaluate historic ISA because the NLCD only has analyses from 1998 through 2011. The tracing method involved obtaining aerial imagery and then uploading the imagery to ArcGIS as a .jpg or .tiff file. The image had no geospatial reference so the user manually oriented the image using the georeferencing tool. The tool anchored the image as the user selected points (vertices) from the original that were a direct match to points (vertices) on the basemap, and as few or as many "anchor points" may be added as desired.

Once, this orientation process was complete the ISA analysis was begun. This included the following steps: (1) tracing all impervious surface in the watershed by hand, (2) classifying the land types of the traced regions by using the classification schema and descriptions shown in figure 2.1.1, (3) calculating the area of the each land type, and (4) multiplying the land type area by the corresponding value for % ISA by land type.

The steps were repeated for both all modern and historical images from the years 1953, 1998, and 2017. A calculation was then performed to find % ISA change within a specific time period. The % ISA change calculation:

$$(\frac{ISA_2 - ISA_1}{ISA_1})100 = \%\Delta$$

Where 1 is the year of the earlier imagery, and 2 is the year of the 2017 imagery. The total % change will reference change (increase or decrease) from the earlier date to the later date.

2.1.3 Woodard and Curran (W&C) Method

The dataset for the Woodard and Curran method was provided to this study by CES Inc. and includes the GIS data that was used to perform the original 22% impervious surface cover estimate by Woodard and Curran (Environmental Consulting). This method was simply a replication of W&C's previous calculation and was achieved by adding the ISC polygon into GIS and calculating the area of the ISC polygon using the statistics function within the attribute table. That polygon was then divided by the total area of the watershed to confirm that the 22% estimate was accurate for the value of total watershed area that had been used in the other two methods: NLCD and Tracing.

2.2 Coring/Subsampling and Radiocarbon Date

The HB-3 (Hart Brook Floodplain) core was taken on October 5, 2017. The core was taken in the largest floodplain in the Hart Brook (shown in fig 2.2.1) at 44° 4'23.60"N, 70°11'29.56"W. It is 150cm long by 5cm in diameter. A cylindrical Dutch corer with no auger was driven into the floodplain to extract the core. Once the corer was driven down as far as possible, it was rotated 6 times in a circle and then pulled out carefully and straight upwards. The core consisted of 4 drives with little to no overlap between drives 1-2 and 2-3. Between drive 3-4 there was approximately 11cm of overlap, but as this could not be definitively validated, all of the data are presented a true, uninterrupted chronologic record. After each drive the core was transferred from the corer into halves of a PVC pipe cut lengthwise. Each drive was wrapped separately in plastic wrap. The other half of the PVC pipe was then placed on top to secure the core and the two half were wrapped together in another layer of plastic wrap. The core halves were designated as one working half and one archive half. Both halves were refrigerated immediately upon return to facilities and the working half was only removed from refrigeration in order to perform core analyses.

The HB-3 core was subsampled 2cc every cm for the first 20cm and then 2cc every 5 cm to the bottom of the core, 150cm. The subsamples were put directly into pre-weighed crucibles. The % water content was determined by weighing the subsamples and crucibles together. The samples and crucibles were then dried and reweighed. Crucible weights were subtracted from both wet and dry weights. The final calculation for % water was the following:

Figure 2.2.1: (FEMA floodplain map) HB-3 Coring Site

[Total wet mass (g) – Total dry mass (g)] / Total wet mass (g) *100 = % Water Content

Next dry bulk density was calculated using the following equation: (All of the values necessary values were already recorded in the procedure for % water content)

[Total dry mass (g) – crucible mass (g)] / 2 (cm^3) = dry bulk density (g/cm^3)

Radiocarbon Date:

A piece of organic material was extracted from between 72-74 cm, the upper clay layer. The sample was a reddish brown wood fragment. The sample was cleaned and sonicated before being sent to DirectAMS Laboratory in Bothell, Washington. There the sample was prepared with an acid-base-acid treatment. Calibrations of radiocarbon ages were done with Calib 7.10 using the calibration dataset: intcal 13.14c.

2.3 Lead Analysis and Dating Model

Lead concentrations were analyzed on soil/sediment every ten cm along the entire HB-3 core. 0.5g of sub-sampled soil and sediment was digested in 10ml of hydrochloric acid to dissolve organic matter and strip metals from the sediment surface. After approximately 15

minutes, they were placed into a high powered microwave and digested according to EPA soil standard settings for method 3051A (see references for link to full details). Samples were left to depressurize for 24hrs. The following day the samples were diluted in 50ml volumetric flasks with E-pure. Approximately 10ml of each sample was transferred into a 15mL plastic test tube and run through ICP – OES.

Lead 2203 wavelength was the most significant and relevant result produced by this analysis to core dating, but additional data for As1937, Cd2288, Cu3273, Fe2599, K_7664, Mg2795, Na5895, Ni2216, and Zn2025 was also collected. The ICP-OES produced results in units of mg/L, which required further correction unless an actual full 1L dilution was used. In the case of this study, dilutions were 50mL. Lead concentrations are also conventionally displayed in units of mg/kg, so the (g) of digested sediment was converted to (kg). The normalization and correction calibration for each sample was the following:

[Lead 2203 (mg/L) * 0.05 (L)] / [Mass of sediment (g) * (kg) / 1000 (g)] = Lead 2203 (mg/kg)

After solving for the "raw" lead concentrations, the normalized lead concentrations were also calculated. Depending upon the type of substrate and comparisons to local baseline lead values, sometimes the raw or normalized data will be preferred. This study will account for and analyze both raw and normalized lead data.

The calculation for lead concentration normalization is as follows:

$$\left(\frac{mg\ Pb}{kg\ sed}\right)\left(\frac{100g\ sed}{x\ g\ C}\right)\left(\frac{kg}{1000\ g}\right) = Normalized\ Lead\ \left(\frac{mg}{gC}\right)$$

2.4 Percent Carbon Content

Samples were run for % Carbon through an EA-c-IRMS in the EGL at Bates College. Elemental analysis was performed using a Costech Analytical brand Elemental analyzer, Model 4010. The analyzer was set up for carbon and nitrogen. Each EA run consisted of one bypass, one blank, nine standards and 38 samples. The three running standards used were in house standards Acetanilide (δ15N -0.49, δ13C -33.89), Caffeine (δ15N -12.23, δ13C -30.92) and a powdered/homogenized cod muscle tissue (δ15N 13.62, δ13C -18.62), all of which have a known isotopic value determined against NIST standards. Mass spectrometry was performed on a Thermo Finnigan Isotope ratio mass spectrometer, model Delta V Advantage and isotopic

ratios were determined using our Isodat 3.0 software. Soil samples were weighed out and the specific mass of each was recorded to normalize the data post-analysis. For organic rich sediments approximately 5-7 mg were analyzed and for inorganic material (clay, sand, and gravel) approximately 15 mg or more were analyzed.

2.5 Magnetic Susceptibility

Magnetic susceptibility (MS) analysis was performed on the HB-3 core at every 1cm interval downcore. This analysis was done using the Bartington MS2E Sensor at a 3.8 mm spatial resolution. The measurements were taken along the core before any invasive analyses were performed. Magnetic susceptibility is an undisruptive analytical technique, so the core was fully viable for other types of analyses afterward. The core was prepared for analysis by gently placing a layer of plastic wrap over the length of the entire core to avoid cross contamination. Readings were taken every 1 cm down the sediment core. A small interval was chosen to detect any nuances within the sedimentary record, but not so small that an unmanageable or unnecessary amount of data was generated.

Magnetic susceptibility measurements describe the amount of the magnetic minerals in each 1cm layer of the core. Magnetic minerals measured are, most commonly, magnetite, titanomagnetite, hematite, and goethite (Enos, 2015 and Hall 1998). The presence of magnetite has an empirical relationship to grain size, and layers with higher amounts of magnetite typically have larger grain size, while layers with lower amounts of magnetite have smaller grain size (Dearing, 1999). Additionally, MS has a relationship to organic material. Higher MS values are typically associated with low organic content, while low MS are associated with high organic content (Dearing, 1999).

2.6 Grain Size Analysis

Approximately 2.5 grams of dried sample from every 10cm downcore were subjected to wet sieving, grain size analysis. Masses were carefully weighed and recorded before beginning. The samples were already broken up, so homogenization was not necessary in this case, but would be otherwise. Subsamples were transferred into 50 mL Oak Ridge plastic, centrifuge tubes and 5 ml of 30% hydrogen peroxide was added to digest any remaining organic material. Distilled water was then added to bring the centrifuge tubes to an even, near-filled level. The tubes were left uncapped in a rack and placed in a Precision Water Bath Model 183, set to 50° C,

for 5 hours to accelerate organic digestion. Tubes were then capped and left in the room temperature bath overnight. The following day, the tubes were placed in an IEC CU-5000 centrifuge at 1500 rpm for 10 minutes, after which clear liquid was carefully decanted without losing solids. Distilled water was then re-added to the tubes to the near-filled level and then the solution was sonically dismembrated by the Vortex Genie to churn up sediments. Tubes were again placed in the IEC CU-5000 centrifuge at 1500 rpm for another 10 minutes. Samples continued this cycle until each was decanted at least three times and sonically dismembrated twice (Enos, 2015).

Finally, the samples were filtered through a series of two sieves, 2mm (gravel) and 45um (sand). The sediments from each size class were dried overnight and weighed. The mass of each size class was divided by the total sample mass to calculate the proportionate composition of each type of sediment, gravel and sand, respectively. The remaining portion was assumed to be silt/clay.

2.7 Water Quality Monitoring

In addition to the water quality data already publically available on Hart Brook (MDEP Reports, 2013, 2014, 2015, MDEP TMDL, 2013, and the Watershed Action Plan, 2007), water quality monitoring continues to be performed by CES Inc, of Lewiston ME annually.

Water Quality Dataloggers were deployed during the summer of 2017 at HB1, HB2, HB4, and HB7 by CES Inc, Lewiston ME. These sites were selected because they had historically low dissolved oxygen concentrations. The respective dataloggers used were an In-Situ Aqua Troll 600 at HB1, Hobo Conductivity and DO Loggers at HB2 and HB4, and a YSI 600XL at HB7. All dataloggers recorded Dissolved Oxygen, both (mg/L) and (% sat), Conductivity (mS/cm), pH, and Temperature (degrees C) every fifteen minutes. Additionally, HB1 recorded water pressure.

Dataloggers required recalibration and maintenance frequently. To access data a field computer was brought to each site approximately every three weeks and the data was downloaded. The status of the dataloggers was also checked every three weeks for healthy battery life, accurate measurements (compared to a handheld YSI WQ meter), and appropriate deployment conditions (i.e. good water flow, no debris accumulation, biofilm). If necessary, the dataloggers were cleaned and redeployed.

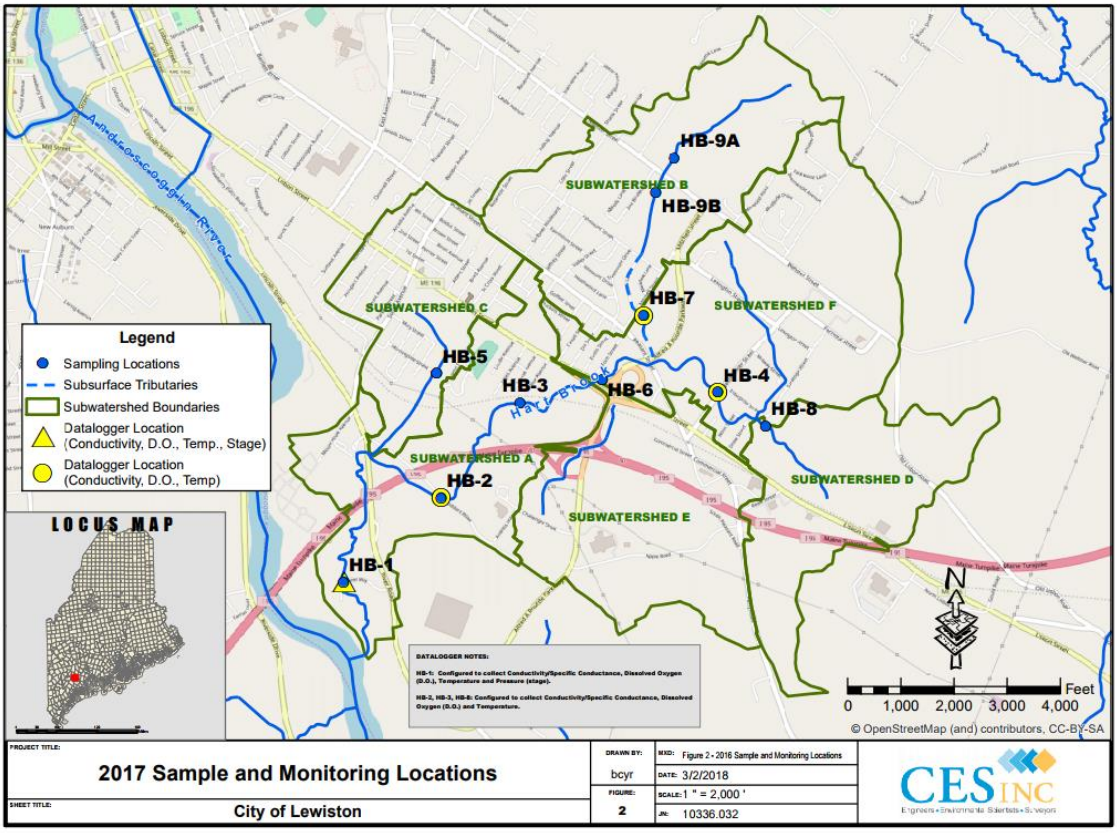

Figure 2.7.1: Hart Brook Water Quality Sampling Sites (CES, Inc.)

3. Results

3.1 Core Description and Radiocarbon Date

The stratigraphy of the HB-3 core was a soil unit, followed by a clay unit, followed by a sandy, gravelly layered unit. The soil unit was a rich, loosely packed, dark brown soil extended from 0-28 cm. The upper 20 cm were heavily rooted and the upper 10 cm had some green, leafy organic material (this material may have been pulled down by the insertion of the auger). Between 28 cm and 54 cm, the soil was more tightly packed and a lighter-brown with fewer roots and little organic material. Between 54 and 79 cm, sediments were dominated by clay with some rusty oxidized coloring. At 59 and between 72 and 74cm organic deposits of wood fragments were found embedded in the clay unit. From 79-83 cm sediments were dominated by sand, but returned to the clay unit from 83-94cm. Between 94 and 150 cm the core then transitioned into sandy, gravelly layers until the end of the core. There were repeating gravel laminae between 104 and 107 cm, 118 and 120 cm, and 129 and 135 cm. These laminae appeared to fine upwards, transitioning from gravel grains to medium grained sand. The fining upward sequence appeared to repeat itself three times.

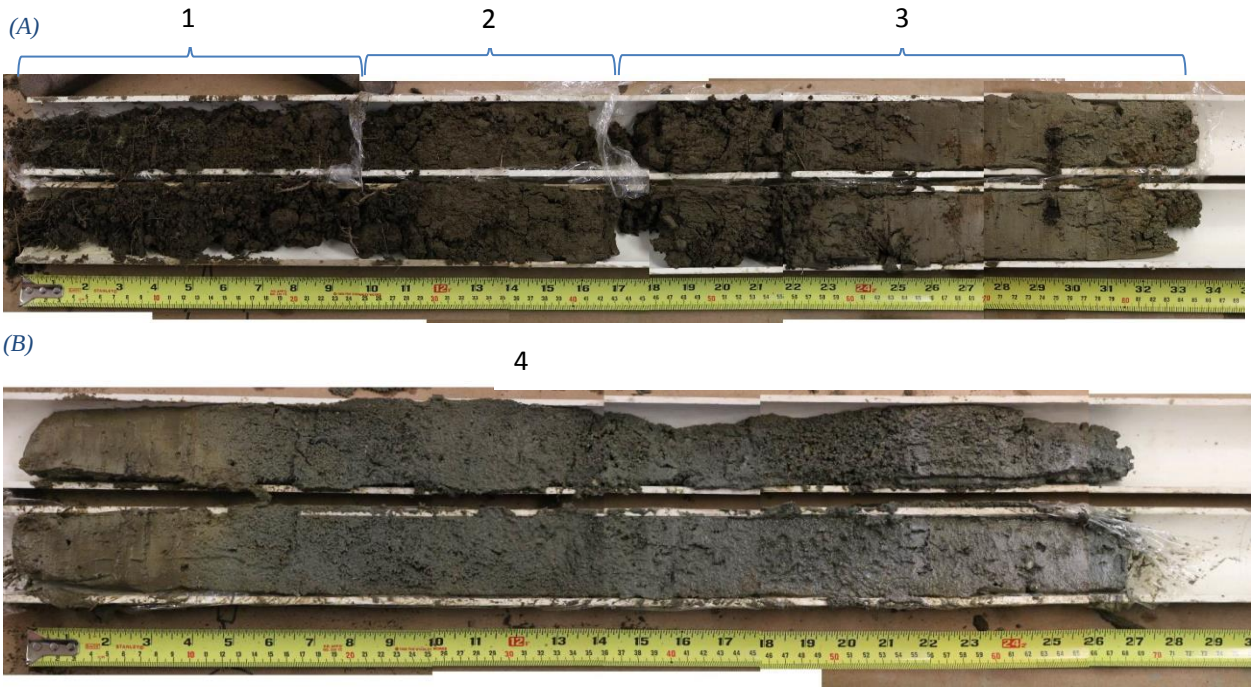

Figure 3.1.1: HB-3 Sediment Core. 150cm in total length. Collected on October 15th, 2017 from Hart Brook floodplain Lewiston, ME. (A) Upper 3 drives (1) 0-25 (2) 25-44 (3) 44-84 cm (B) 4th drive (4) 84-150cm. No overlap existed between drives 1-2 and 2-3. Approximately 11cm of overlap may have existed between drives 3-4 but analyses were performed as if the entire core represented a true, uninterrupted chronologic record.

Radiocarbon Dating:

The wood fragment sample from 72-74 cm sent to DirectAMS lab for radiocarbon dating returned a modern age (1950 or younger).

3.2 Carbon Content

The percent (%) carbon content values were highest in the organic soils near the surface and lowest in the clay, sand, and gravel layers (Fig. 3.2.1). Carbon content decreased quickly between 0 and 30cm, then slowly between 30 and 60cm. From 60-65 there was a sharp decline, and, finally, values remained below 1% through the end of the core, 150cm. The largest value for % carbon content was 6.5% at 0cm, while the smallest was 0.4% at 150cm.

Dry bulk density is almost a mirror image of % carbon content and shows a clear trend of increasing density with increasing depth, a rather intuitive conclusion as sediment continues to accumulate above and compact the sediment layers below. Density values plateaued around 100cm and hovered at approximately 1.5-2.0 g/cm^3 through the end of the core. Overall, density increased down-core regardless of changing stratigraphy and did not appear to be heavily influenced by the type of substrate.

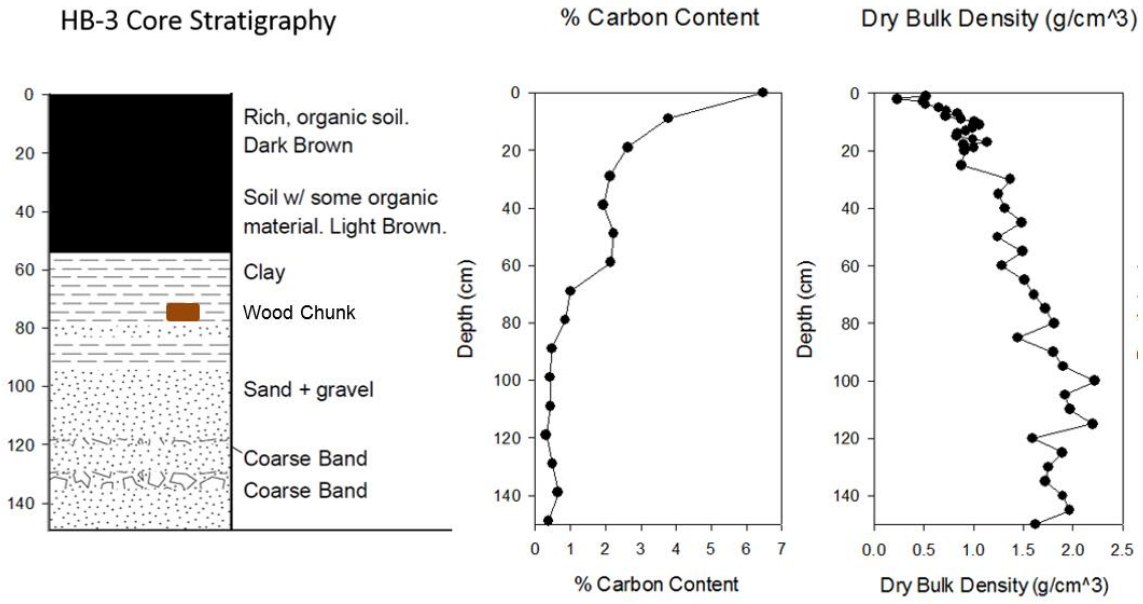

Figure 3.2.1: Carbon content and dry bulk density

3.3 Core Water Content

The % water content values showed a clear peak at 60 cm (fig. 3.3.1), 50%, the maximum value for the dataset. There was a gradational stratigraphic change beginning at 55cm from soil and sand to clay. It is worth noting and considering the close proximity of the % water content peak and the beginning of the clay layer. Additionally, the dry bulk density (shown in fig 3.2.1) continued to increase throughout the peak % water content, likely reflecting the amount of available pore space. Clay has low permeability which does not transport water easily. An additional spike in water content was present at 85cm, where the core returned to sandy material before the values dropped into clay and then sand and gravel.

The minimum value for % water content, 17%, occurred at 120cm. Therefore, the total range of % water content was 28 %. Unlike dry bulk density, the lowest values appeared consistently at the bottom of the core, rather than the top. There was no simple, linear relationship between dry bulk density and % water content, so a closer look at the stratigraphy and geochemistry of the core was also needed. The lowest values at 120cm and 140cm lay directly at the base of the aforementioned gravel laminae and have high proportions of gravel. Here permeability and the abundant pore space would allow water to drain from the sediment more easily.

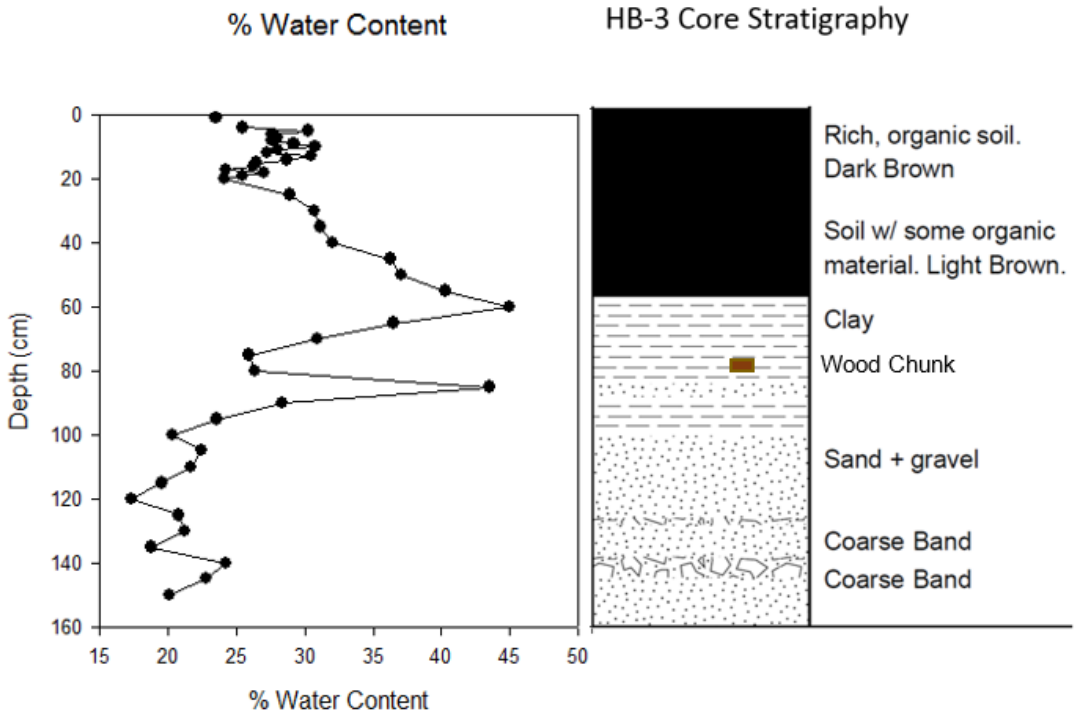

Figure 3.3.1: Percent (%) water content and stratigraphy

3.4 Core Magnetic Susceptibility

Magnetic susceptibility is a measure of the amount of magnetic minerals (most commonly magnetite) present in a sample of sediment or soil. The amount of magnetite is also positively correlated to grain size and inversely correlated to the amount of organic matter within a sample. Larger grains will have higher MS, while organic material will contain lower. That said, it is difficult, if not impossible, to parse out the exact relative proportional influence of those three variables. For example, if the sample at 20 cm had a low magnetic susceptibility value, which it did, is that an indication of high organic content or small grain size or low magnetic mineral content? It becomes evident that, in this case at 20 cm, the overwhelming factor would be the presence of organically rich soil. A detailed understanding of the substrate or core being analyzed is needed to use magnetic susceptibility measurements effectively.

This sample showed a positive correlation between depth and magnetic susceptibility. As seen in the % water content results, the gravel laminae were also visible within this dataset. High magnetic susceptibility values correlated to the coarsest laminae found at approximately 120 and 140cm. The minimum value, -23.1, occurred at 2 cm. The maximum value, 7, occurred at 112 cm. Values appeared to have the most variability between 15 and 50 cm, while above and, especially, below the values had less standard deviation.

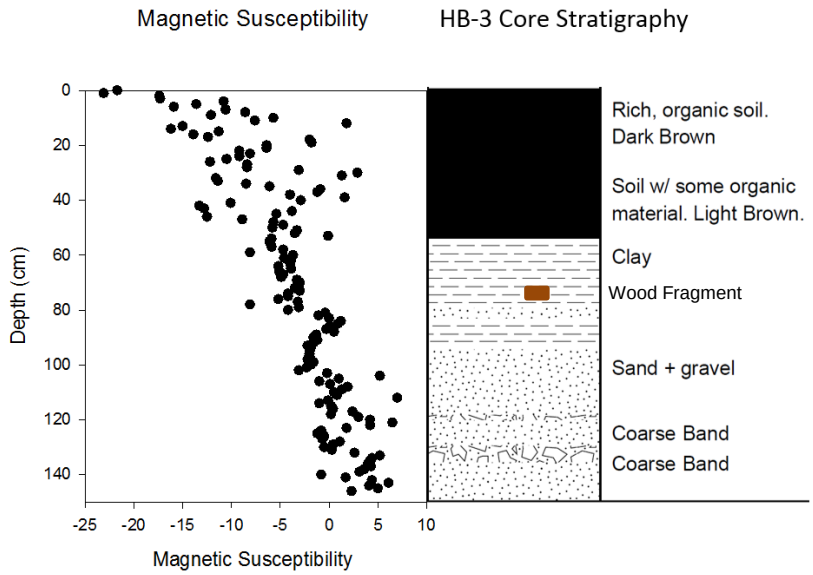

Figure 3.4.1: Magnetic susceptibility and stratigraphy

3.5 Lead Analysis

Lead analysis was performed in an effort to constrain the timing and extent of sedimentation. There was a clear peak in lead concentration at approximately 40cm, before and after which the concentrations increased or decreased, respectively, for both the normalized and raw lead data. The rates of increase or decrease in lead concentration were steep. In the raw data, from 0 to 40cm the slope was 0.59 (mg/kg)/cm, and from 40 to 70 the slope was - 1.33 (mg/kg)/cm. If the peak in lead concentrations is assumed as the year 1972, the year leaded gasoline was outlawed and the genesis of most American-based lead concentration decline in soil (Callender, 2004), than the average sedimentation rate from 1972-2017 is equal to 0.85 cm/yr.

Baseline concentrations of lead, 15.3 mg/kg or less in Appalachian soils (Saint-Laurent et al., 2010), appear to begin at approximately 60 cm in reference to the raw data and continue through the end of the core at 150cm, but the normalized data does not show a clear return to baseline. If the raw data were to be assumed a chronologic record, that would place 60cm as the onset of the burning of leaded gasoline in approximately 1923 (Callender, 2004). If the normalized data are taken to be an accurate chronology, than the entire core must be assumed modern with no natural lead levels present.

In the raw data, the minimum value 2.91 mg/kg occurred at 120 cm. Therefore, the total range of lead concentrations was 46.7 mg/kg. It is also worth noting that the peak in lead concentration occurs at 40cm, well above the beginning of the clay layer at approximately 54cm. Also, the trend of lead concentration appears to occur independent of changes in dry bulk density or % water content.

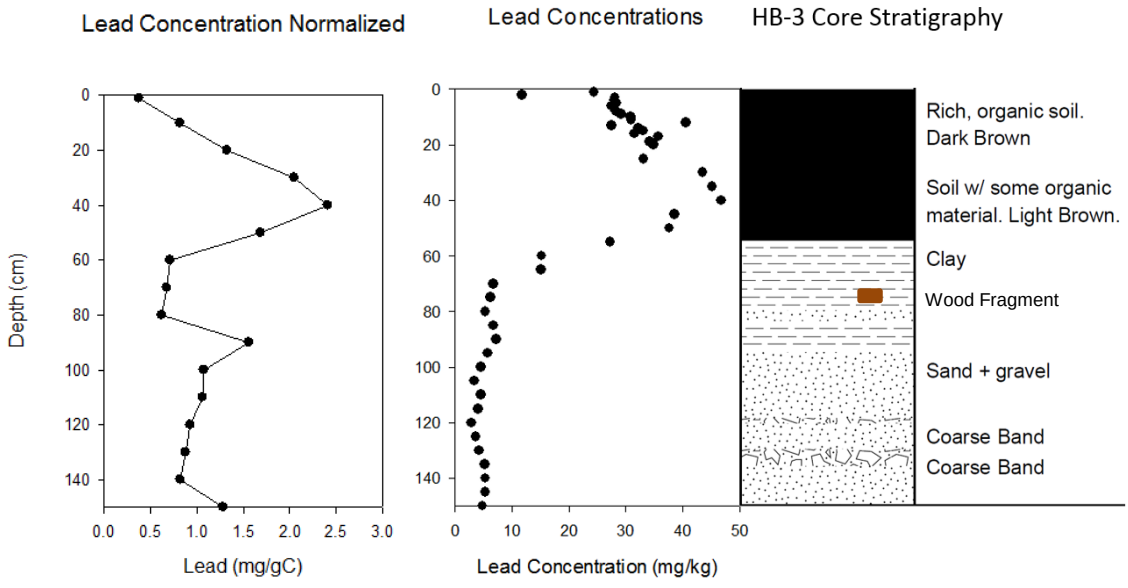

Figure 3.5.1: Lead concentration normalized and raw with stratigraphy

3.6 Grain Size

Grain size results showed a clear stratigraphic change at 100 cm. Above 100cm samples were predominantly silt and clay with some sand but no gravel. Subsamples below 100cm had lower levels of silt and clay, higher levels of sand, and some gravel. This change matched well with the core description, but also provided additional evidence of stratigraphic changes and a quantitative analysis of grain size. The accompanying table 3.6.1 shows grain size percent distribution and aligns the data with its corresponding core depth.

The % gravel values ranged from 0 - 10%, with a maximum at 110 cm. Sand ranged from 27% at 60cm to 76 % at 100cm. Mud ranged from 22% at 110 cm to 73% at 60 cm.

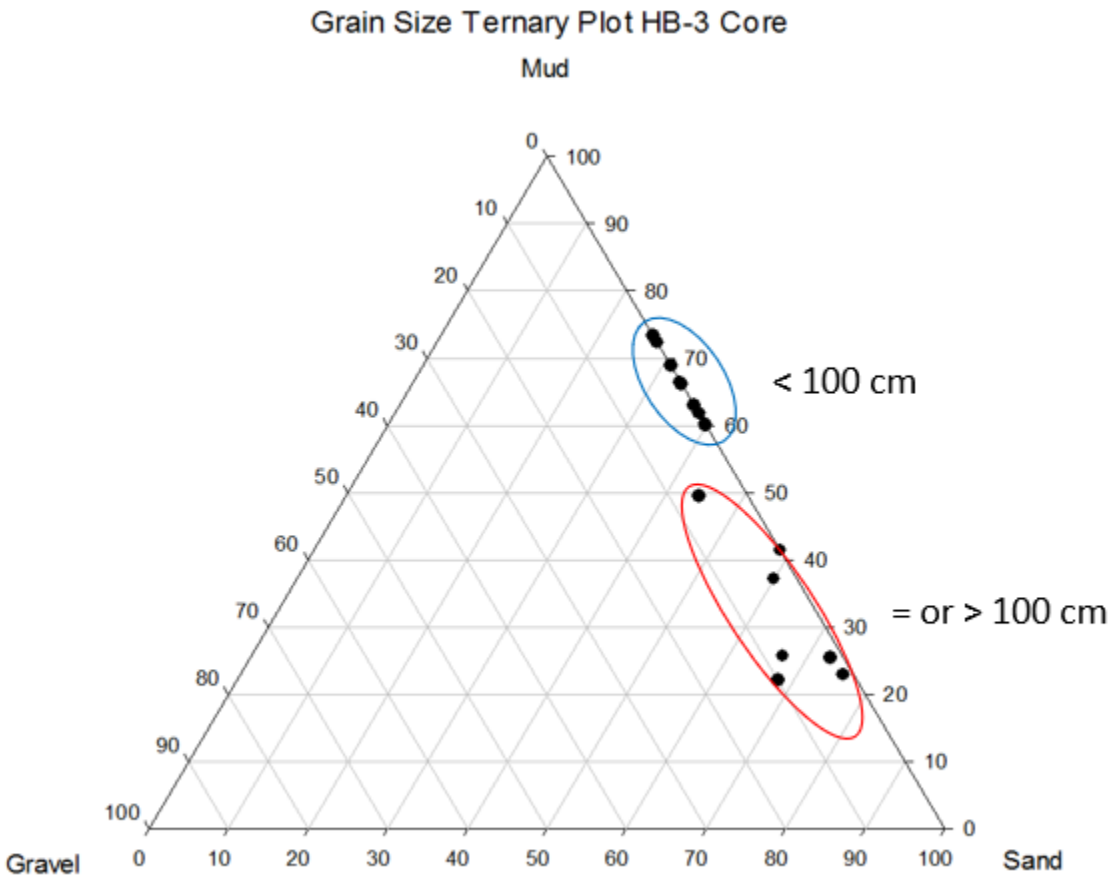

Figure 3.6.1: Ternary plot showing grain size distribution. Mud, sand, and gravel.

Table 3.6.1: Grain Size Distribution HB-3 Core

Depth	Total Mass (g)	Dry Mass Sand (g)	Dry Mass Gravel (g)	Dry Mass Silt/Clay	% Sand	% Gravel	% Silt/Clay
1	2.5331	0.9680	0	1.5651	38	0	62
10	2.9895	1.1946	0	1.7949	40	0	60
20	2.1464	0.8542	0	1.2922	40	0	60
30	2.7403	1.0150	0	1.7253	37	0	63
40	2.7703	0.9298	0	1.8405	34	0	66
50	2.5277	0.7869	0	1.7408	31	0	69
60	2.9607	0.7908	0	2.1699	27	0	73
70	2.7071	0.7494	0	1.9577	28	0	72
80	2.164	1.2687	0	0.8953	59	0	41
90	2.2517	0.7629	0	1.4888	34	0	66
100	2.6904	2.0381	0.0363	0.6160	76	1	23
110	2.2899	1.5583	0.2262	0.5054	68	10	22
120	2.0022	1.3372	0.1508	0.5142	67	8	26
130	2.9403	2.1449	0.0475	0.7479	73	2	25
140	2.6117	1.5656	0.0751	0.9710	60	3	37
150	2.1365	0.9488	0.1318	1.0559	44	6	49

3.7 Spatial Analysis

Three methods were used to calculate impervious surface cover within the Hart Brook watershed based upon different needs and limitations of historic imagery. The goals of this section are to re-estimate impervious surface area and calculate the rate of urbanization in the watershed over time.

NLCD Method: The first method, which used data sorted by land development type from the National Land Cover Dataset, quantified 1% of the watershed as developed open space, 6% as low intensity development, 14% as medium intensity, 12% as high intensity, and finally 0.04% as Barren Land. Added together, percent impervious surface cover yielded a total of 33% for the Hart Brook Watershed. The HB-4 (industry) sub-watershed and near the mouth of the river had the highest density of dark red or high intensity development (see Table 3.7.1 for color classification schema.

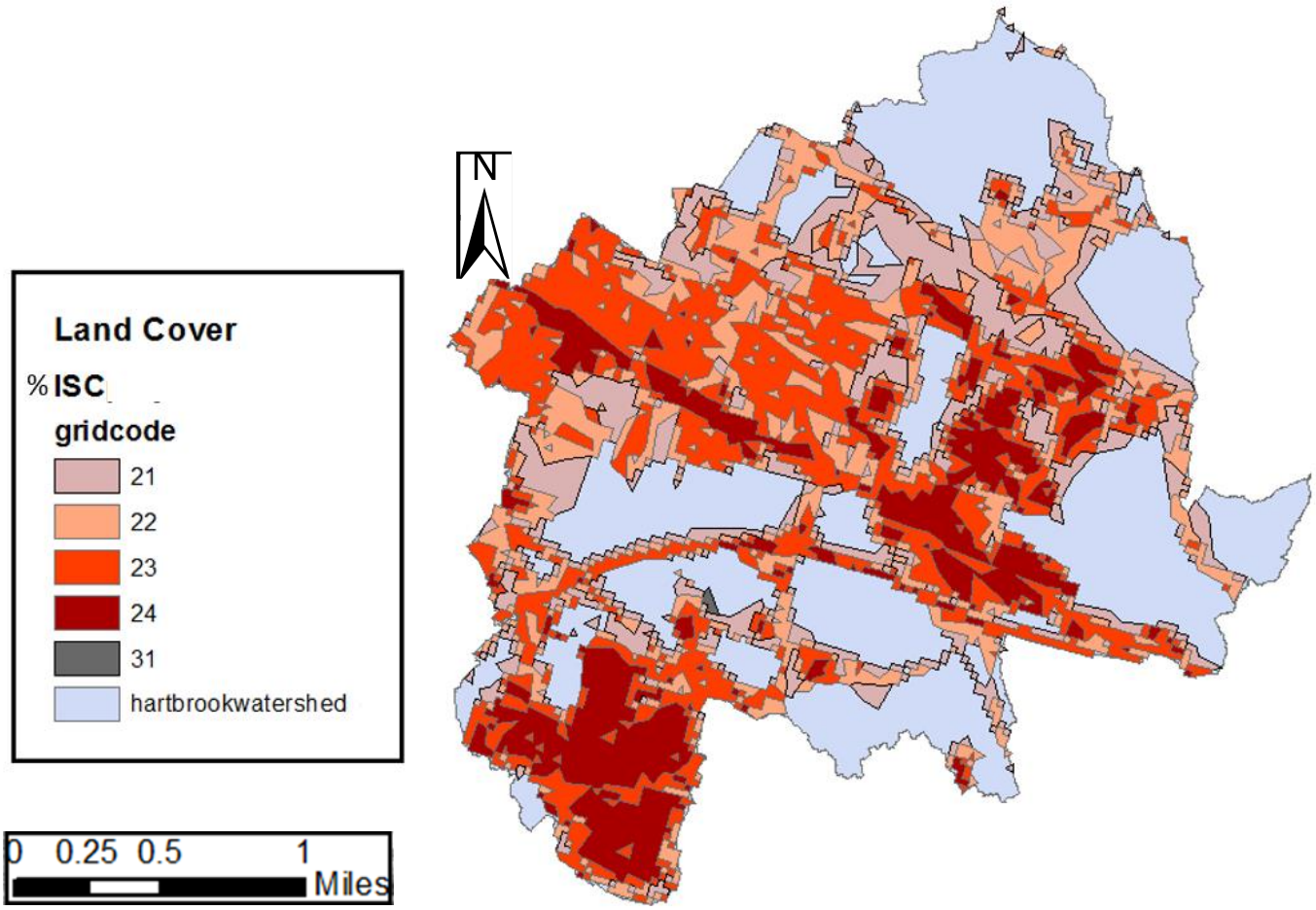

Figure 3.7.1: Map and legend of National Land Cover Dataset Impervious development in Lewiston, ME, Hart Brook Watershed

Table 3.7.2: Method 1, National Land Cover Dataset % ISC

Grid Code	Land Type	Area Developed	%ISC for Land Type	Area ISC	Watershed Area	%ISC	Total % ISC
21	Developed, Open Space	1,180,016	0.1	118,002	8,933,060	1	33
22	Low Intensity Development	1,457,014	0.35	509,955	8,933,060	6	
23	Med Intensity Development	1,913,129	0.65	1,243,534	8,933,060	14	
24	High Intensity Development	1,178,925	0.9	1,061,032	8,933,060	12	
31	Barren Land	4,289	0.85	3,646	8,933,060	0.04	

Developed	
21	**Developed, Open Space** - areas with a mixture of some constructed materials, but mostly vegetation in the form of lawn grasses. Impervious surfaces account for less than 20% of total cover. These areas most commonly include large-lot single-family housing units, parks, golf courses, and vegetation planted in developed settings for recreation, erosion control, or aesthetic purposes.
22	**Developed, Low Intensity** - areas with a mixture of constructed materials and vegetation. Impervious surfaces account for 20% to 49% percent of total cover. These areas most commonly include single-family housing units.
23	**Developed, Medium Intensity** - areas with a mixture of constructed materials and vegetation. Impervious surfaces account for 50% to 79% of the total cover. These areas most commonly include single-family housing units.
24	**Developed High Intensity** -highly developed areas where people reside or work in high numbers. Examples include apartment complexes, row houses and commercial/industrial. Impervious surfaces account for 80% to 100% of the total cover.
Barren	
31	**Barren Land (Rock/Sand/Clay)** - areas of bedrock, desert pavement, scarps, talus, slides, volcanic material, glacial debris, sand dunes, strip mines, gravel pits and other accumulations of earthen material. Generally, vegetation accounts for less than 15% of total cover.

Table 3.7.1: Legend of land NLCD land classifications for Fig 3.7.1

Tracing-by-Hand Method: This study used a second methodology to calculate land cover which involved tracing developed areas on high resolution aerial photographs and satellite imagery. The purpose of this method was to calculate change in pervious surfaces over time, which would later be compared to rates of sedimentation over time. This technique was used on a historic aerial image of the Hart Brook Watershed from 1953 and satellite imagery from 1998 and 2017. The results yielded very low values of % impervious surface cover in 1953, approximately 7.5 % ISC.

Two permutations were run to calculate the impervious surface cover of the 2017 imagery. One presumed that the entire traced ISC watershed area was medium intensity development (65% ISC), and the other assumed that half of the traced area was medium intensity development (65% ISC) and the other half was high intensity development (90% ISC). As defined by the National Land Cover Dataset, medium intensity development contains "areas with a mixture of constructed materials and vegetation. Impervious surfaces account for 50-79% of the total cover. These areas most commonly include single-family housing units." In the Hart Brook Watershed, 100% medium intensity development can be considered a low end estimate for 2017, while in 1953 it was likely a more suitable classification. Today, the Hart Brook watershed includes industrial complexes, multifamily homes, apartment complexes, and even a major interstate. It likely has some degree of high intensity development, defined as, "highly developed areas where people reside or work in high numbers. Examples include: apartment complexes, row houses, and commercial/industrial development. As defined by the NLCD "Impervious surfaces account for 80-100% of the total cover," in high density development

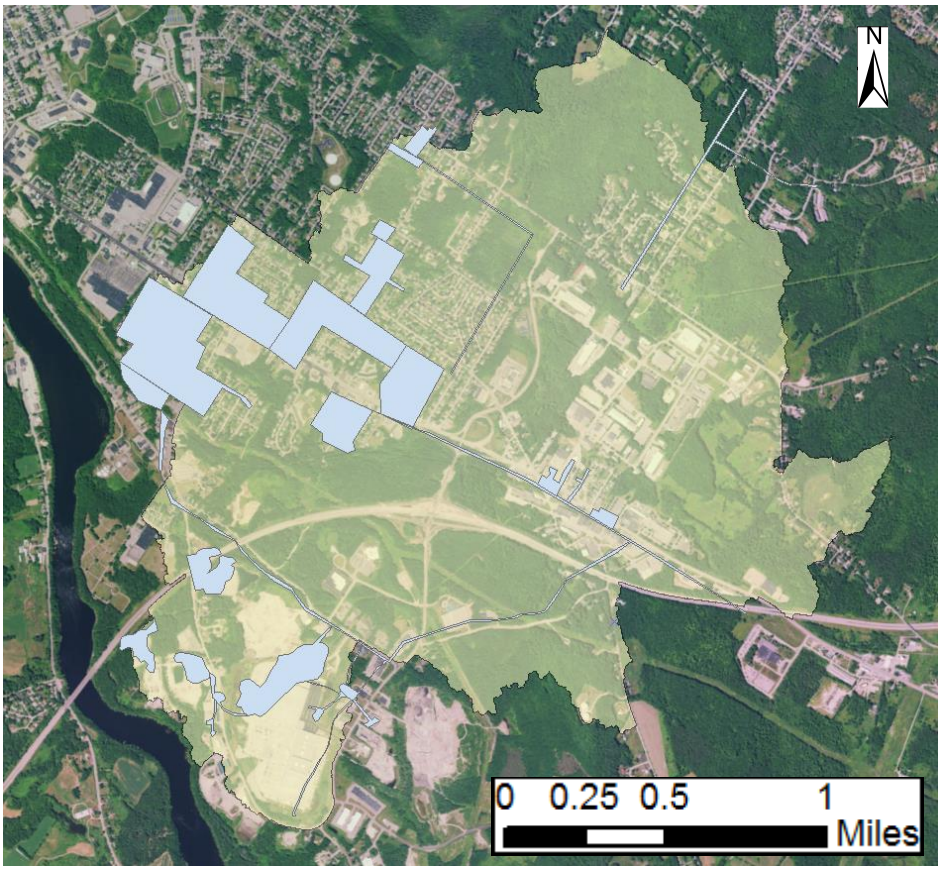

Figure 3.7.2: 2017 aerial imagery with 1953 tracing overlain.

areas. The calculations for the 2017 imagery projected that impervious surface accounts for 25 % of the watershed, if all development is classified as medium intensity, and 30%, if half of the development is classified as medium intensity and half of the development is classified as high intensity. These are rough estimates as the classification schema used was not originally intended for this method and there is opportunity for human tracing-error. The broad intention was, moreover, to attain a general sense of the rate of development over time.

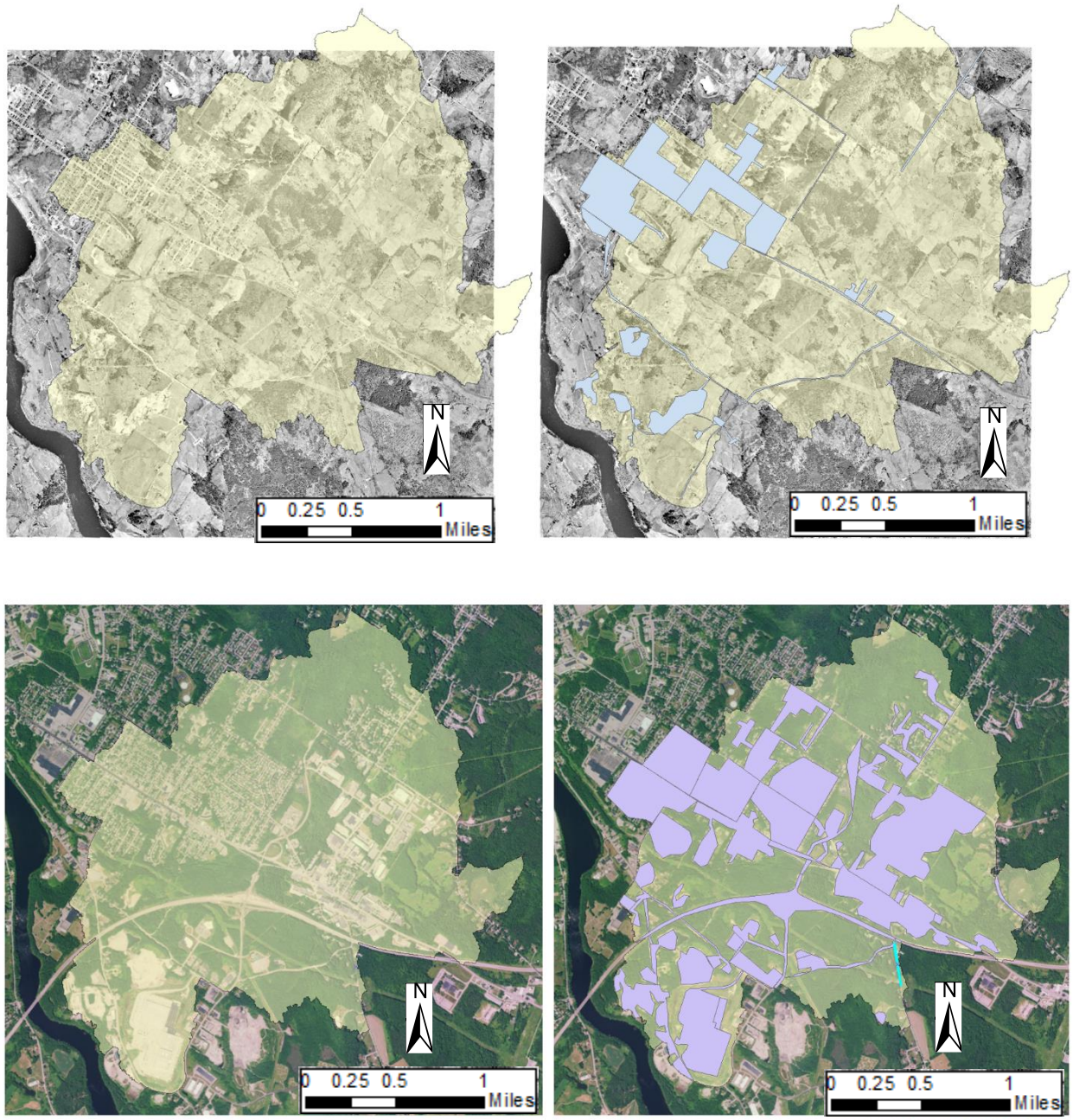

Figure 3.7.3: (Above) 1953 imagery with of Hart Brook watershed, Right, with development traced. (Below) 2017 imagery with of Hart Brook watershed, Right, with development traced.

In either case, the Hart Brook watershed has experienced extreme change in land cover and a rapid rate of urbanization between 1953 and 2017, 64 years. The % change in impervious surface cover showed a 335% or a 400% increase in permutations 1 and 2, respectively. In other words, there is between 3 and 4 times the amount of impervious cover in 2017 as there was in 1953.

To provide further constraints on development rate a 1998 aerial imagery was analyzed (Fig 3.7.4), and it was discovered that there was essentially no change in impervious surface cover between 1998 and 2017. The only slight visible change was, surprisingly, a reduction in the size of the Pike Industries quarry in the southernmost tip of the watershed. For further analyses and comparison, the area of development between 1998 and 2017 will be assumed 0 m^2. This 1998 image was not traced individually, as it was nearly identical to the 2017 development. Analyses on the 2017 images, particularly the NLCD calculation, can be assumed accurate for all years between 1998 and 2017. A main goal of the spatial analysis portion of this study is to reform rather than update the previous estimation of impervious surface cover performed by W&C in 1998.

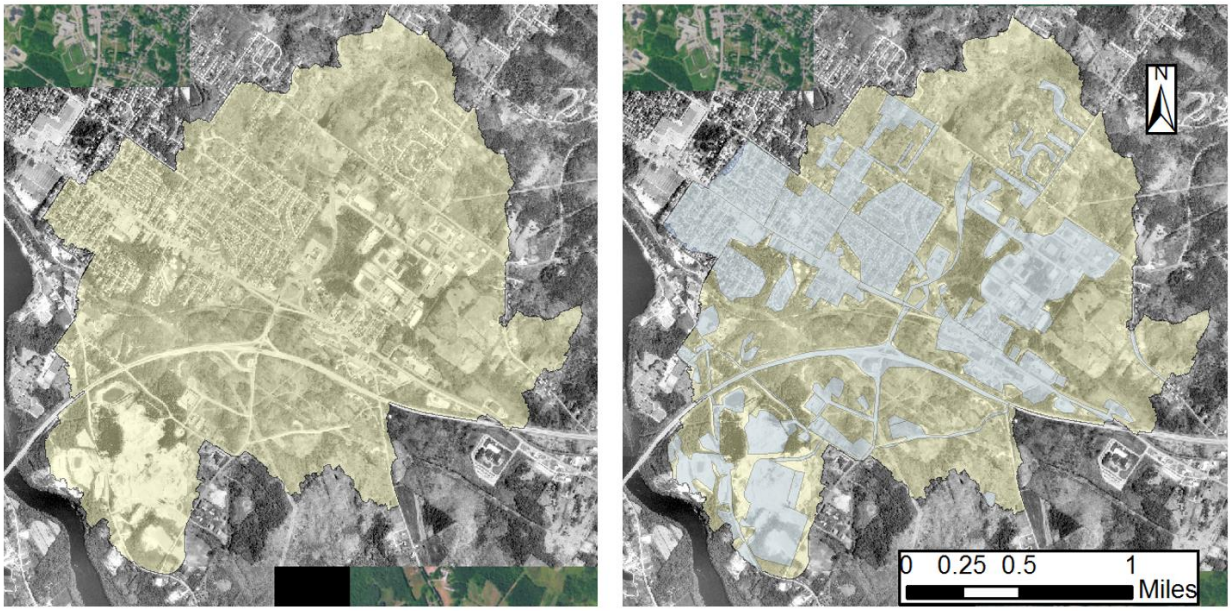

Figure 3.7.4: (Left) 1998 Imagery (Right) 1998 Imagery with 2017 ISC tracing overlain shows no change in overall development area.

Fig 3.7.3, on the previous page, is the 1953 tracing overlaying the 2017 aerial imagery (which has the same total area of development as in 1998) and visually emphasizes the large extent of expanding development. Between 1953 and 1998, the average annual increase in ISC was 39,634 m^2. For scale, that is 7.4 entire American football fields of pure impervious surface added to the watershed each year. The equations were the following:

1. [Total ISC (m^2) $_{1998}$ – Total ISC (m^2) $_{1953}$] / Number of Years (1998-1953)
   = development per year (m^2)
2. development per year (m^2) / area of a football field (m^2)

Table 3.7.3: Method 2, Development Tracing Comparative % ISC Calculations, 1953 and 2017. The second row (1953) is compared to 2017 data in rows (3) and (4 and 5 collectively). Row 3 represents all ISA in 2017 as medium intensity development. The sum of rows 4 and 5 represent the total ISA in 2017 when impervious surfaces are considered half medium and half high intensity development.

Row	**Year**	Area Developed	Development Type	% Cover for Type	Total ISC	Total watershed area	% ISC	Total %ISC	% Change (1953-2017)
2	1953	1,028,000	Med. Intensity	65	668,200	8,933,060	8	8	
3	2017	3,441,000	Med. Intensity	65	2,236,650	8,933,060	25	25	335
4	2017	1,720,500	Half Med. Intensity	65	1,118,325	8,933,060	13	30	399
5	2017	1,720,500	Half High Intensity	90	1,548,450	8,933,060	17		

W&C Method:

The recalculation of Woodard and Curran data yielded 22% impervious surface cover. Methods remain unknown and some sections of impervious area appear left untraced, like the compact substrate within the Pike Industries industrial park (southernmost tip of the watershed), occasional rooftops and thin roadways.

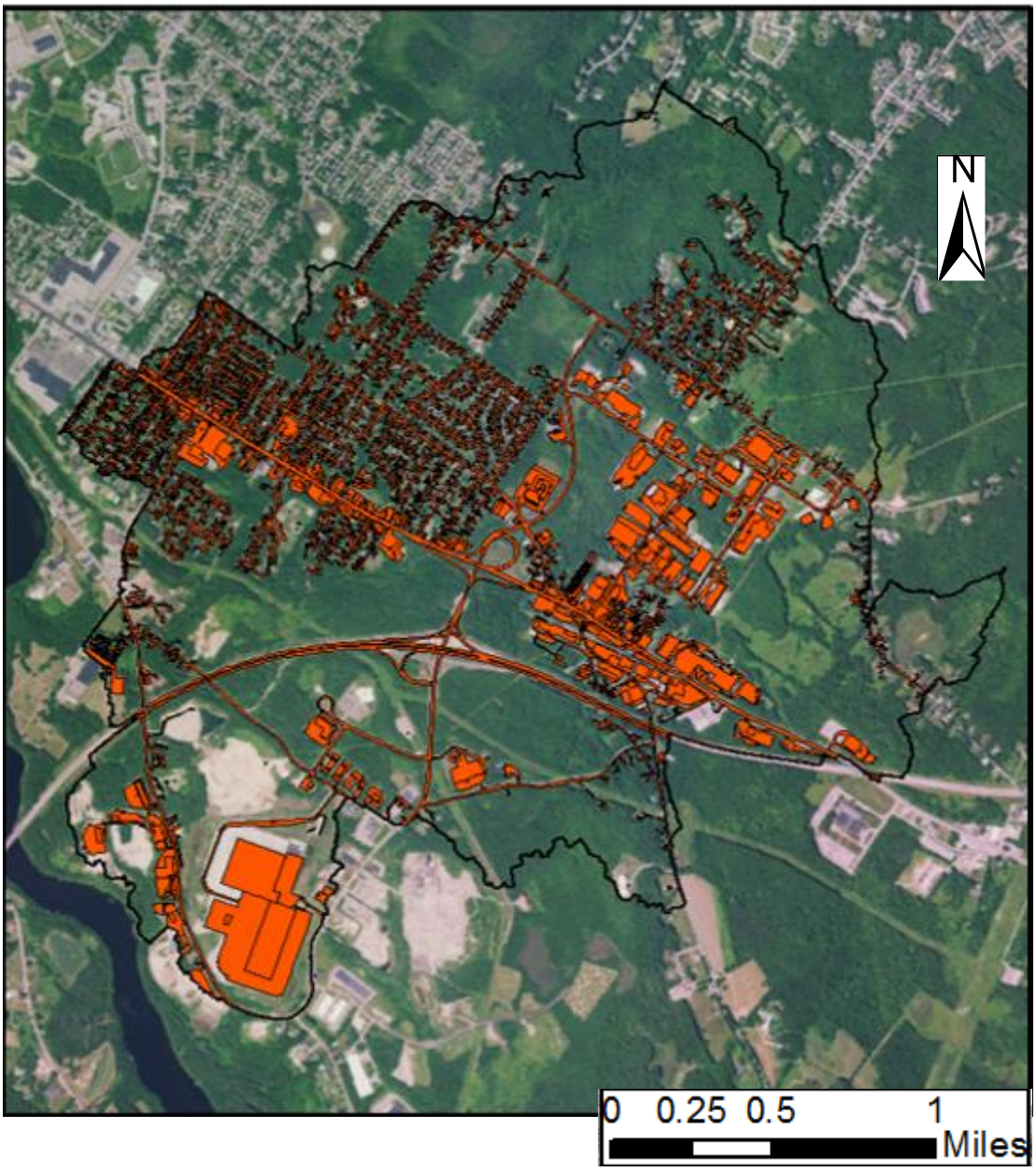

Figure 3.7.5 Woodard and Curran Method

3.8 Water Quality: Temp and D.O.

Recent water quality results show a trend of increasing temperature throughout the summer season. In 2017, the median values were lowest during July 27, 2017 sampling at approximately 17.5°C. By August 23, 2017, values increased by approximately 2°C to 19.5°C, and remained similarly high, 19.5°C, in late September (Sep, 27). In both August and September, the HB-4 sampling site had, by far, the highest temperatures. It is worth recognizing that the HB-4 industry sub-watershed also had the highest levels of impervious surface.

Levels of dissolved oxygen were also measured during those same sampling events, and an opposite, declining trend was apparent throughout the summer season. In July the overall median dissolved oxygen level of all the sites hovered around 7mg/L ,the class B state requirement (MDEP), or just above. HB-4, as well as HB-6, HB-8 HB-and 9A, fell below that standard. In August, the median value remained just above 7mg/L, but many more sites fell below 7mg/L including HB-2, HB-4, HB-6, HB-8, HB-9A, and HB9-B. Measurements were taken twice that day, once in the morning and once in the evening. Late September (Sep, 27) sampling measured a median value of less than 6mg/L, well below the state standard, and each site failed to reach the requirement at least once during the day. Again, measurements were taken twice, morning and evening.

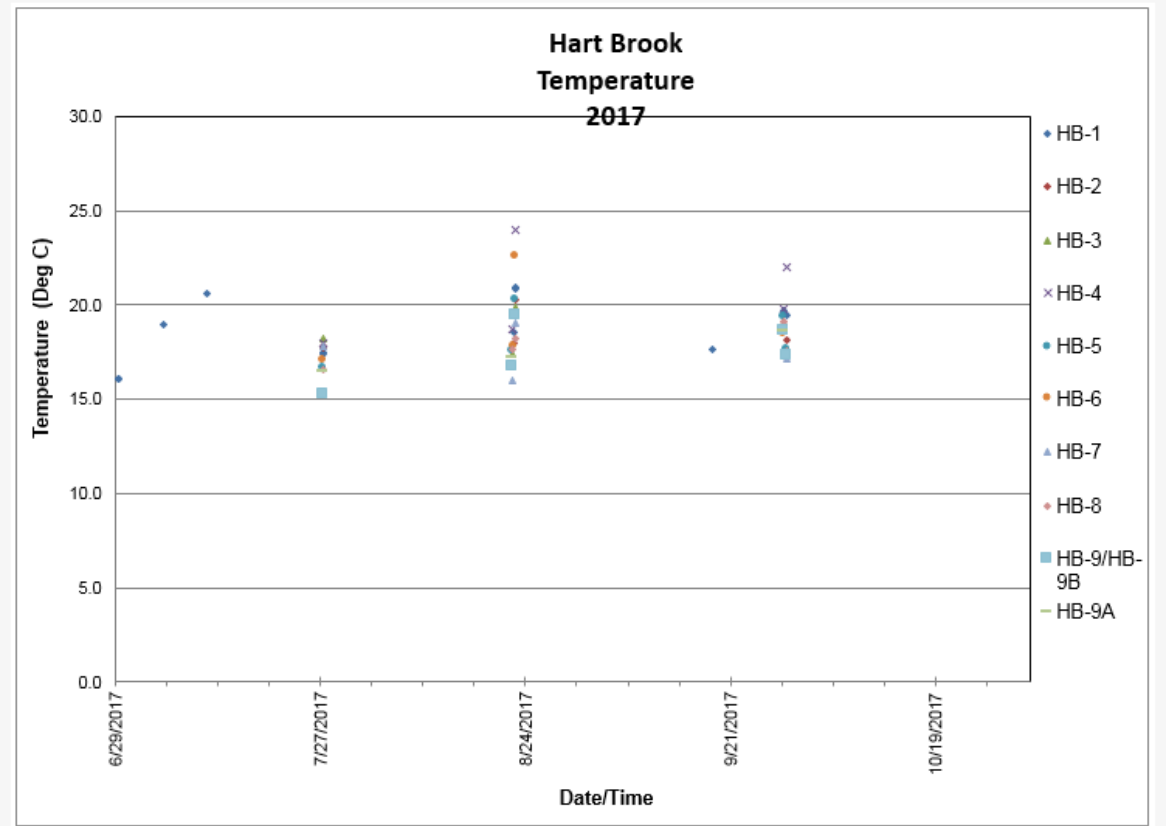

Figure 3.8.1: Summer 2017 Temperature Hart Brook (CES Inc.)

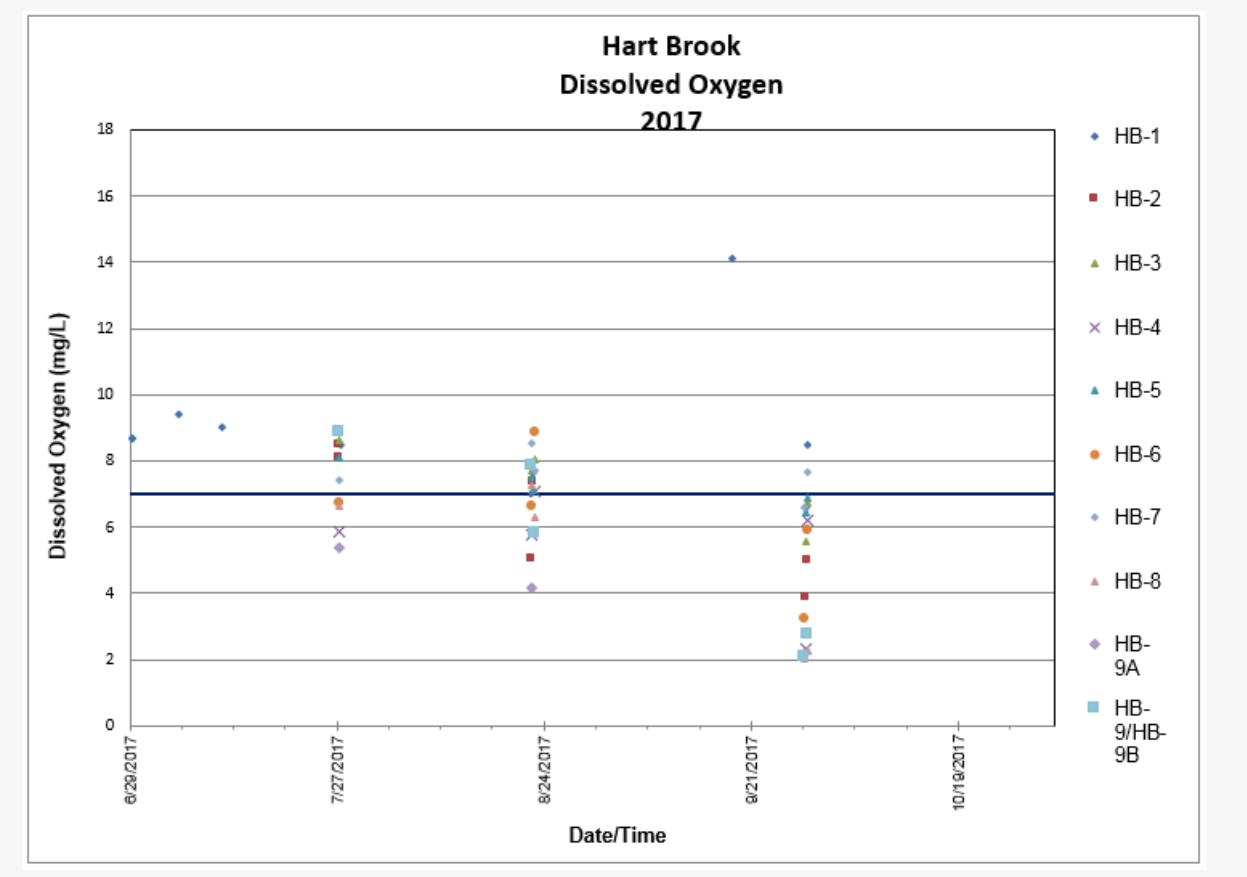

Figure 3.8.2: Summer 2017 Dissolved Oxygen (mg/L) Hart Brook (CES Inc.)

Barometric pressure was found on the same days as summer sampling (see table 3.8.1). The following equation was used to convert from pressure in inHg to mmHg:

mmHg value x 133.322 Pa = inHg value x 3386.39 Pa.

Using Henry's Law the pressure and temperature values on these given dates can be used to calculate the expected value of dissolved oxygen in equilibrium with the atmosphere (see Fig 3.8.4 and column six of Table 3.8.1).

Table 3.8.1: Temperature, pressure, and dissolved oxygen data for Hart Brook Summer 2017

Date:	Avg. Water Temperature (°C)	Pressure (inHg)	Pressure (mmHg)	Avg. Measured Dissolved Oxygen (mg/L)	Expected Dissolved Oxygen at Equilibrium Conditions (mg/L)
7/27/2017	17.5	29.57	751.1	7.2	9.4
8/23/2017	19.5	29.4	746.8	7.2	9.0
9/27/2017	19.5	29.57	751.1	6.0	9.0

Table 3.8.1, is a summary table of all of the above stated information (Radtke et al, 1998). The importance of these calculations is to compare measured levels of dissolved oxygen with expected values of dissolved oxygen at specific conditions. Any discrepancy between these two figures indicates that an outside factor (likely biologic activity) is causing the system to shift out of equilibrium (Radtke et al, 1998). All of the above differences between measured and expected D.O. are significant, 2.2, 1.8., and 3.0 for July, August, and September, respectively.

Table 3.8.2: Temp and Pressure Effect on D.O. Hart Brook: Solubility of oxygen in water at various temperatures and pressures (Radtke et al, 1998)

Temp	Atmospheric pressure, in millimeters of mercury																		
°C	795	790	785	780	775	770	765	760	755	750	745	740	735	730	725	720	715	710	705	700
15.0	10.5	10.5	10.4	10.3	10.3	10.2	10.1	10.1	10.0	9.9	9.9	9.8	9.7	9.7	9.6	9.5	9.5	9.4	9.3	9.3
15.5	10.4	10.4	10.3	10.2	10.2	10.1	10.0	10.0	9.9	9.8	9.8	9.7	9.6	9.6	9.5	9.4	9.4	9.3	9.2	9.2
16.0	10.3	10.2	10.2	10.1	10.0	10.0	9.9	9.8	9.8	9.7	9.7	9.6	9.5	9.5	9.4	9.3	9.3	9.2	9.1	9.1
16.5	10.2	10.1	10.1	10.0	9.9	9.9	9.8	9.7	9.7	9.6	9.5	9.5	9.4	9.4	9.3	9.2	9.2	9.1	9.0	9.0
17.0	10.1	10.0	10.0	9.9	9.8	9.8	9.7	9.6	9.6	9.5	9.4	9.4	9.3	9.3	9.2	9.1	9.1	9.0	8.9	8.9
17.5	10.0	9.9	9.9	9.8	9.7	9.7	9.6	9.5	9.5	9.4	9.3	9.3	9.2	9.2	9.1	9.0	9.0	8.9	8.8	8.8
18.0	9.9	9.8	9.8	9.7	9.6	9.6	9.5	9.4	9.4	9.3	9.3	9.2	9.1	9.1	9.0	8.9	8.9	8.8	8.7	8.7
18.5	9.8	9.7	9.7	9.6	9.5	9.5	9.4	9.3	9.3	9.2	9.2	9.1	9.0	9.0	8.9	8.8	8.8	8.7	8.7	8.6
19.0	9.7	9.6	9.6	9.5	9.4	9.4	9.3	9.3	9.2	9.1	9.1	9.0	8.9	8.9	8.8	8.8	8.7	8.6	8.6	8.5
19.5	9.6	9.5	9.5	9.4	9.3	9.3	9.2	9.2	9.1	9.0	9.0	8.9	8.9	8.8	8.7	8.7	8.6	8.5	8.5	8.4
20.0	9.5	9.4	9.4	9.3	9.3	9.2	9.1	9.1	9.0	8.9	8.9	8.8	8.8	8.7	8.6	8.6	8.5	8.5	8.4	8.3
20.5	9.4	9.3	9.3	9.2	9.2	9.1	9.0	9.0	8.9	8.9	8.8	8.7	8.7	8.6	8.6	8.5	8.4	8.4	8.3	8.3
21.0	9.3	9.2	9.2	9.1	9.1	9.0	8.9	8.9	8.8	8.8	8.7	8.6	8.6	8.5	8.5	8.4	8.4	8.3	8.2	8.2
21.5	9.2	9.2	9.1	9.0	9.0	8.9	8.9	8.8	8.7	8.7	8.6	8.6	8.5	8.4	8.4	8.3	8.3	8.2	8.1	8.1
22.0	9.1	9.1	9.0	9.0	8.9	8.8	8.8	8.7	8.7	8.6	8.5	8.5	8.4	8.4	8.3	8.2	8.2	8.1	8.1	8.0
22.5	9.0	9.0	8.9	8.9	8.8	8.8	8.7	8.6	8.6	8.5	8.5	8.4	8.3	8.3	8.2	8.2	8.1	8.0	8.0	7.9
23.0	9.0	8.9	8.8	8.8	8.7	8.7	8.6	8.6	8.5	8.4	8.4	8.3	8.3	8.2	8.1	8.1	8.0	8.0	7.9	7.9
23.5	8.9	8.8	8.8	8.7	8.6	8.6	8.5	8.5	8.4	8.4	8.3	8.2	8.2	8.1	8.1	8.0	8.0	7.9	7.8	7.8
24.0	8.8	8.7	8.7	8.6	8.6	8.5	8.4	8.4	8.3	8.3	8.2	8.2	8.1	8.0	8.0	7.9	7.9	7.8	7.8	7.7
24.5	8.7	8.7	8.6	8.5	8.5	8.4	8.4	8.3	8.3	8.2	8.1	8.1	8.0	8.0	7.9	7.9	7.8	7.7	7.7	7.6
25.0	8.6	8.6	8.5	8.5	8.4	8.3	8.3	8.2	8.2	8.1	8.1	8.0	8.0	7.9	7.8	7.8	7.7	7.7	7.6	7.6
25.5	8.5	8.5	8.4	8.4	8.3	8.3	8.2	8.2	8.1	8.0	8.0	7.9	7.9	7.8	7.8	7.7	7.7	7.6	7.6	7.5
26.0	8.5	8.4	8.4	8.3	8.3	8.2	8.1	8.1	8.0	8.0	7.9	7.9	7.8	7.8	7.7	7.6	7.6	7.5	7.5	7.4
26.5	8.4	8.3	8.3	8.2	8.2	8.1	8.1	8.0	8.0	7.9	7.8	7.8	7.7	7.7	7.6	7.6	7.5	7.5	7.4	7.4
27.0	8.3	8.3	8.2	8.2	8.1	8.0	8.0	7.9	7.9	7.8	7.8	7.7	7.7	7.6	7.6	7.5	7.5	7.4	7.3	7.3
27.5	8.2	8.2	8.1	8.1	8.0	8.0	7.9	7.9	7.8	7.8	7.7	7.7	7.6	7.5	7.5	7.4	7.4	7.3	7.3	7.2
28.0	8.2	8.1	8.1	8.0	8.0	7.9	7.9	7.8	7.7	7.7	7.6	7.6	7.5	7.5	7.4	7.4	7.3	7.3	7.2	7.2
28.5	8.1	8.0	8.0	7.9	7.9	7.8	7.8	7.7	7.7	7.6	7.6	7.5	7.5	7.4	7.4	7.3	7.3	7.2	7.1	7.1
29.0	8.0	8.0	7.9	7.9	7.8	7.8	7.7	7.7	7.6	7.6	7.5	7.5	7.4	7.3	7.3	7.2	7.2	7.1	7.1	7.0
29.5	8.0	7.9	7.9	7.8	7.8	7.7	7.6	7.6	7.5	7.5	7.4	7.4	7.3	7.3	7.2	7.2	7.1	7.1	7.0	7.0

4. Discussion

4.1 Sedimentation Models

Lead concentrations in natural (pre-industrial < 1923) soils have a mean value of approximately 15.3 mg/kg for the Appalachian geological region (Saint-Laurent et al., 2010), the region within which the Hart Brook resides. 15.3 mg/kg is well above the baseline concentration in the raw lead dataset of this study, which are approximately 4 mg/kg between 60 and150 cm. This suggests that that portion of the core represents natural sediment/soils. Additional evidence that the lead concentrations in the Hart Brook are natural below 60cm was their similarity to baseline lead values found in Taylor Pond, a local waterbody only a few miles from the watershed. Eberle (2008) found baseline lead concentrations in Taylor Pond to be approximately 1.46 +/- 0.22 mg/kg.

It is important to note that non-normalized lead concentrations (mg/kg) began to increase steeply at approximately 70cm, but values are still considered baseline between 60-70 cm both because they are below 15.3 mg/kg and because the normalized lead data does not begin its peak until 60 cm. The normalized lead data is considered valid between 0-70cm, but below 70 cm as concentrations drop and remain below 1% carbon content and may exaggerate any variability between 70 and 150 cm.

All that said, a modern age was returned for a radiocarbon sample at 74cm, indicating that 74cm depth is modern (>1950). The two sources of evidence, lead dating and radiocarbon dating, do not align. If the lead concentration data indicated that 1923 was at 60cm, than a radiocarbon date younger than 1923 could not exist at 74cm. This initial evidence was puzzling, but it was also far from inconclusive. Multiple theories can be entertained and each will have its own implications for interpretation. Three theories have been developed that emphasize different aspects of the geochemical and paleo-environmental data collected. This section of the discussion will tease out the details of the three separate theories and compare them to one another in order to draw conclusions. The following are the three sedimentation models:

1. Modern Sedimentation: The sedimentation is all representative of urbanization and modern processes, and the entire core is younger than 1923.
2. Holocene Sedimentation: The lower portion of the core was deposited by a late glacial shallow marine environment and the uppermost 65cm are the modern recontinuation of sedimentation after a significant unconformity.
3. Historical Sedimentation: The lead age-dating model is used for the uppermost 60 cm and an average sedimentation rate is applied to the bottom 60-150cm.

Two dates will be important to remember throughout the discussion. The role of leaded gasoline in soil records was referenced in the introduction of this study, but these dates must be made explicit. 1923 is the year that the onset of burning of leaded gasoline began to rapidly increase lead concentrations in soil. 1972 is the year that the Clean Air Act banned leaded gasoline and concentrations in soil began a steep decline. These distinct anthropogenic alterations of natural soil evidenced in the lead record will allow for the dating of specific depths within the HB-3 sediment core and, further, the extrapolation of sedimentation rates. They are a fundamental tenant of each of the three following sedimentation models.

Modern Sedimentation (1923-present):

For the first theory, this model will depend upon the radiocarbon date and the normalized lead data, but not the raw lead data. Variations in lead concentrations throughout the lowermost 60-150 cm of the core will be considered to have been caused by human activity related to lead use, and none of the core will be treated as natural or preindustrial. This implies that the entire core is younger than 1923.

There are a few immediate implications of such a young sediment core. First of all, this would mean that there has been a significant amount of sedimentation in the past century. The minimum rate would be approximately 2.4 cm/yr from 1923 until 1972 (assuming the base was exactly the year 1923, but it may be younger). The rate would reduce to 0.85 cm/yr. from 1972 until 2017. If the bottom of the core never returned to baseline, which can be an interpretation of the normalized lead concentration data, then this theory holds true. Such rapid sedimentation could easily be a product of intense development, particularly during the 40s and 50s within the watershed.

Each sedimentological unit would have had a distinct paleo environment specific to the modern-core theory. The fining upward sequences would not show enough geologic time for there to be the depositional sequence of a shifting stream channel or point bar. Instead, these units would have to have been flooding events within the brook, where a pulse of storm water and enough energy input would have caused sediments to overtop the stream banks and be carried from higher elevations to the floodplain. The coarse grains would have been the first to settle out, then sands, and finally clay; hence, the use of the term: fining upward sequence.

The overlaying clay layer may have formed by the ponding of water for a significant portion of time after a flooding event and is likely comprised of reworked marine clay from the late Pleistocene. Despite the much older parent material, the dates of any organic inclusions, like perhaps the wood radiocarbon date from 74cm, would not be representative of the original date of the marine clay (approximately 11,000 years ago). Young organic inclusions could exist in this environment.

Finally, the uppermost layers of soil are evidence of organic colonization and the dilution of inorganic sediments by the increasing presence of organic material. This portion of the core represents relative stability compared to the underlying flooding sequences, and a drier environment than the ponding-clay layer. In order for there to be a significant amount of soil present, there has likely not been recent flooding to the extent of the earlier sand and gravel layers, otherwise the soil may have been stripped away and developed vegetation uprooted.

The connection between the modern sedimentation theory and urbanization or development is indicated by the shear amount of sediment that would need to have been deposited in the last 94 years, which is 1.5 meters. The highest rate of sedimentation correlates well with the highest rate of development, 2.24 cm/yr and the equivalent of 7.4 football fields of ISA added to the watershed annually. Clearly, though, more work is needed. The rate of 2.4 cm/yr extends back in time farther than 1953, when development rates are accounted for, and would have been high before development began in the watershed if ISA trends were extrapolated further. It is possible that sedimentation may have been even more rapid than 2.24 cm/yr at the height of development and slowed toward the beginning of the 20th century, but no evidence or constraints are provided to make that argument.

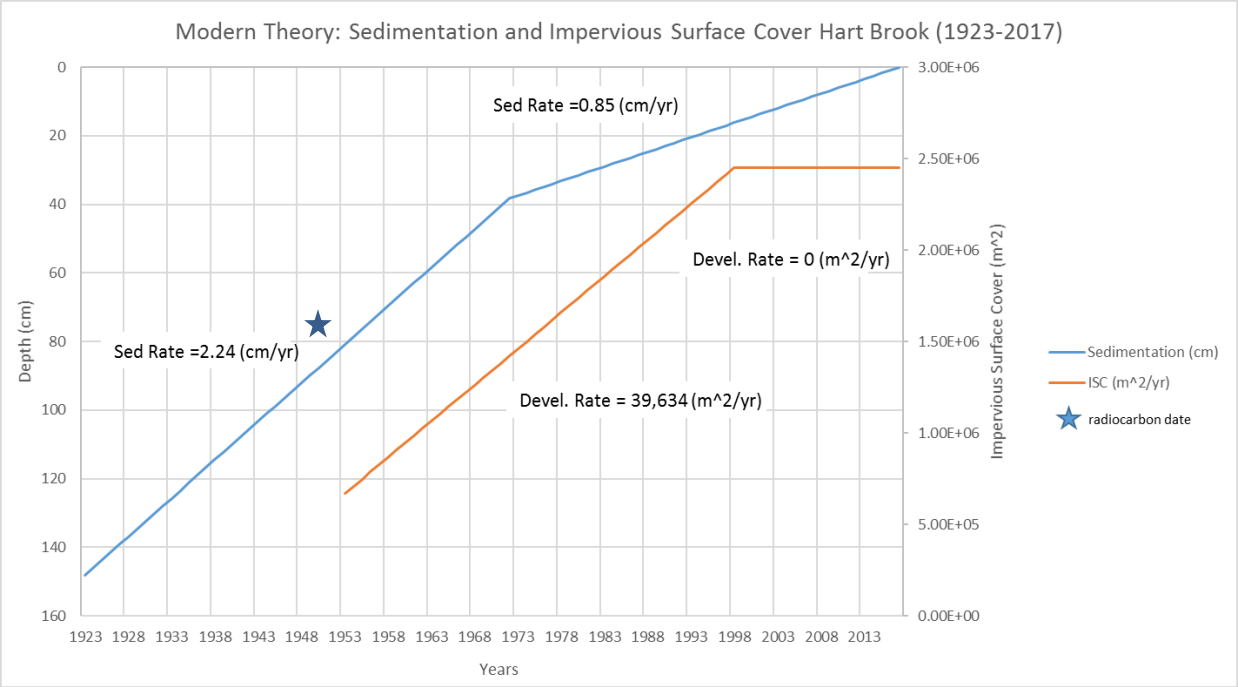

Figure 4.1.1 Modern Sedimentation Theory: Sedimentation and ISC from 1923-2017

Holocene Sedimentation:

The Holocene sedimentation theory has a comparable amount of supporting evidence to the modern core theory, but necessitates viewing the data in an entirely different light. This theory will emphasize the raw lead concentration data and minor aspects of the normalized lead data, but not the radiocarbon date. The theory proposes that the lower 65-150cm of the core (the sand/gravel and clay units) were deposited by late-glacial meltwater pulses and marine deposition. After the sand/gravel and clay sedimentological units were deposited, there was a longstanding unconformity (though no clear sharp stratigraphic boundary or unconformity exists in the sediment core). Finally, the uppermost 65 cm (the soil unit) were deposited by the modern restarting of sedimentation in the early 1900s generated by a rapidly urbanizing watershed.

In this case, by looking at the raw lead data and normalized data, the onset of lead deposition begins at approximately 60 cm (as described above). The increase in concentrations is exceptionally clear, and the conclusion can be drawn that 60cm correlates to the onset of burning leaded gasoline in approximately 1923. At a similar depth, the clay layer begins to grade into soil. There is no sharp boundary, but this may still be an unconformity that has been reworked at the top by recent depositional processes. This signifies that such a substantial amount of modern development and construction was occurring that the amount of runoff increased enough to transport soils and organic material from higher elevation to the floodplain.

Like the modern-core theory, the Holocene theory also has characteristic sedimentological units. The deepest unit in both depth and time is the sand and gravel fining upward sequences. These units would have been created by meltwater pulses from a nearby glacial margin. Upon investigation of glacial maps of the Lewiston area (Hildreth, 2002) a glacial marine delta lay just southeast of the Lake Auburn and may have been the source of meltwater and sediment. The surficial geologic map of Maine identifies the predominant units within the watershed as Ha, braided stream alluvium of late Pleistocene age, and Pmrs, marine regressive sand deposits of Pleistocene age. Ha was more thoroughly described as "fluvially deposited sand, silt, or gravel and occasional muck on terraces cut into glacial

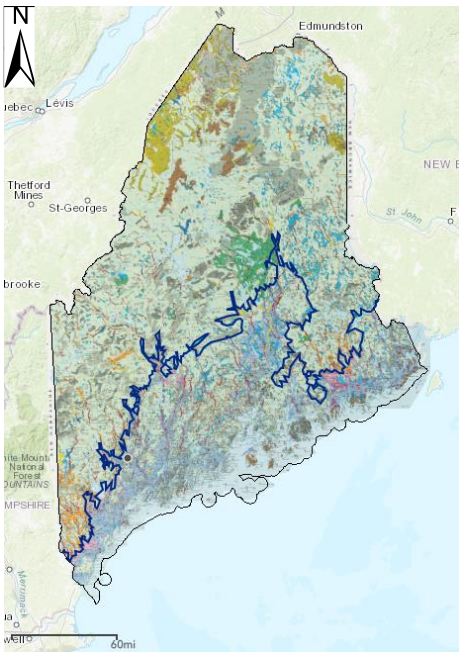

Figure 4.1.2: MGS Surficial Geologic Map of Maine with maximum sea extent

deposits in the Androscoggin River valley…These terraces formed during late-glacial time as sea level regressed' (Hildreth, 2002). Pmrs is described as, "sand, silt, and minor gravel," and it "consists of reworked marine delta, outwash, and bottom materials redistributed by marine currents and wave action as sea level fell during late-glacial time" (Hildreth., 2002). Sequentially, it makes sense that the margin of the glacier would have deposited gravel and sand first through meltwater channels, but where did the clay and silt come from?

As glaciers of the area continued to retreat, the next stage of sedimentation would have aligned with the marine transgression prior to isostatic rebound. The environment would have deposited the marine-clay unit. Fig 4.1.2, shows that the elevation of the clay unit falls within the scope of maximum sea level extent during the Pleistocene, which would have been at approximately the 200ft contour on the historical map of Lewiston (Fig. 4.1.5). Most of the Hart Brook watershed should have some evidence of marine deposits except for occasional and isolated sections of artificial fill surrounding interstate I-95 and within the industrial sub- watershed (see fig 4.1.4).

Upon further retreat and regression, the marine deposits eventually formed a terrace. This would mark the beginning of a longstanding unconformity in the sedimentary record, where there was no deposition or sedimentation and only erosional processes. If this core is considered to be of glaciomarine origin, sedimentation would not occur again until the watershed reached a "tipping point". This study proposes that that tipping point is intimately related to urbanization and development within the watershed. When a large enough volume of runoff (flowing over impervious surfaces) was generated, sediments would be transported from higher elevation to the floodplain. This erosion is only possible when there is a significant energy input, and will not occur if a large proportion of precipitation is percolating down through the soil and sediment to become groundwater. The uppermost 65 cm would be modern sedimentation, beginning in the late 9th or early 20th century, generated by this urbanization.

The Holocene theory provides evidence for urbanization in a different form than the modern sedimentation theory. In this case, the restarting of sedimentation after a conformity argues for the onset of high energy events that had enough strength to mobilize and transport sediments from the upper watershed to the floodplain. As Klein (1979) discovered increases in impervious surface cover often lead to increases in the volume of and flowrates of runoff, which can subsequently accelerate erosional processes. The evidence against this theory is that, although it may have been reworked, there is no visible, sharp boundary between the sand and clay layers, and the radiocarbon date is discounted and would had to have been a root that had grown down into the substrate if the raw lead data is trusted.

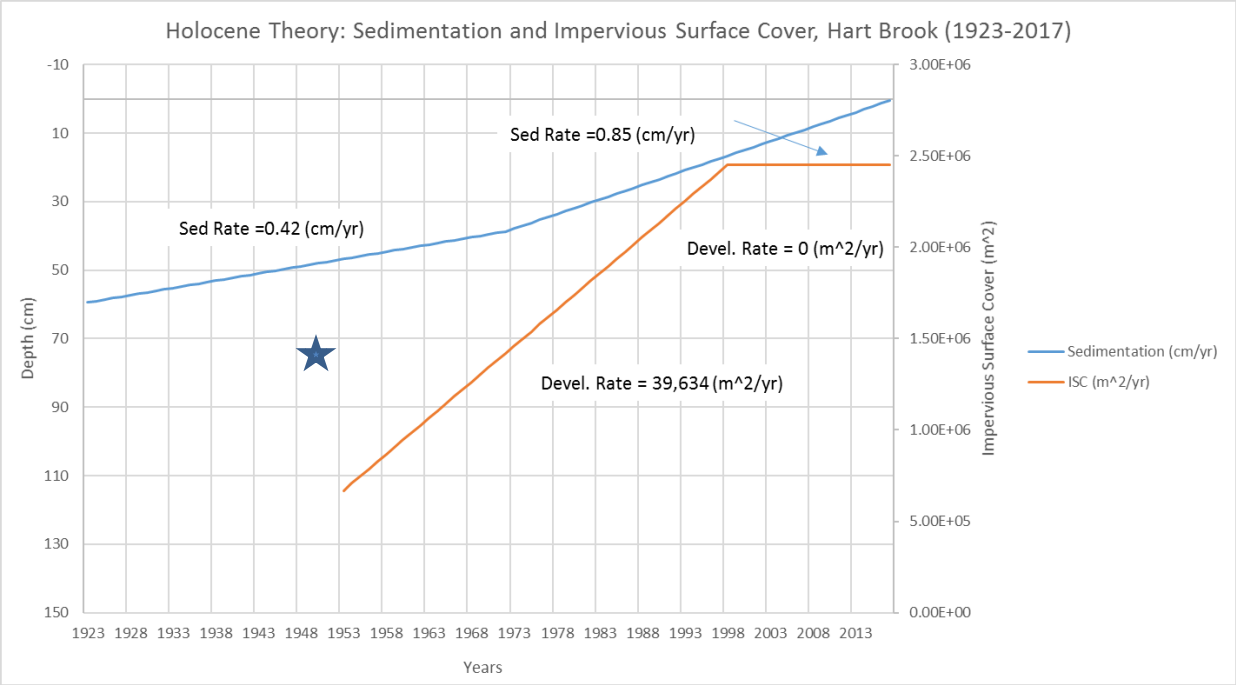

Figure 4.1.3 Holocene Sedimentation Theory: Sedimentation and ISC from 1923-2017. This age model only corresponds to the upper 60 cm of the core.

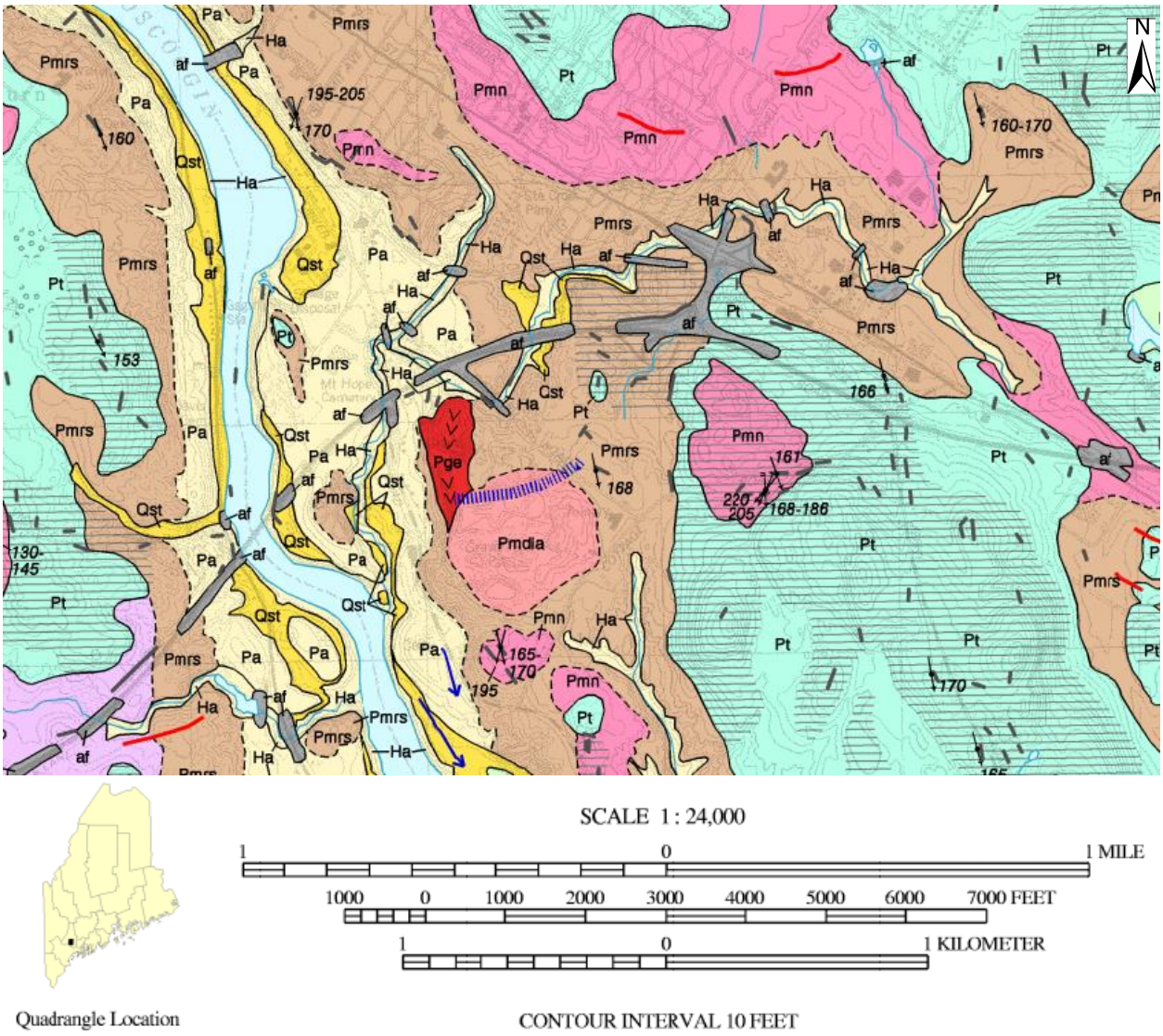

Figure 4.1.4: MGS Surficial Geologic Map of Maine showing the study area, Hart Brook watershed (Hildreth, 2002)

NOTE: A very thin, discontinuous layer of windblown sand and silt, generally mixed with underlying glacial deposits by frost action and bioturbation, is present near the ground surface over much of the map area but is not shown.

af — **Artificial fill** - Man-made. Material varies from natural sand and gravel to quarry waste to sanitary landfill, including highway and railroad embankments and dredge spoil areas. This material is mapped only where it can be identified using the topographic contour lines or where actually observed. Minor artificial fill is present in virtually all developed areas of the quadrangle. Thickness of fill varies.

Ha — **Stream alluvium** (Holocene) - Sand, silt, gravel, and muck in flood plains along present rivers and streams. As much as 3 m (10 ft) thick. Extent of alluvium indicates most areas flooded in the past that may be subject to future flooding. In places, this unit is indistinguishable from, grades into, or is interbedded with freshwater wetlands deposits (Hw).

Hw — **Freshwater wetland deposit** (Holocene) - Muck, peat, silt, and sand deposited in poorly drained areas. Generally 0.5 to 3 m (1 to 10 ft) thick, but may be much thicker in large bogs. In places, this unit is indistinguishable from, grades into, or is interbedded with stream alluvium (Ha).

Qst — **Stream terrace deposit** (Holocene and Late Pleistocene) - Sand, silt, gravel, and occasional muck on terraces cut into glacial deposits in the Androscoggin River valley. These terraces are the lowest recognizable in the valley and were formed in part during late-glacial time as sea level regressed. They are the lowest fluvial terraces in the quadrangle. From 0.5 to 5 m (1 to 15 ft) thick.

Qe — **Eolian deposit** (Holocene and Late Pleistocene) - Fine- to medium-grained, well-sorted sand. Found as small dunes on a variety of older glacial deposits. Deposited after late-glacial sea level regressed from the area and left many fine-grained marine sediments exposed to wind erosion and transport before vegetation established itself and anchored the deposits. Many more thin dunes are present in the area than are delineated on the map. Thickness varies from 0.5 to 8 m (1 to 25 ft).

Qf — **Alluvial fan deposit** (Holocene and Late Pleistocene) - Small fan-shaped deposits of variably sorted sand, gravel, and mud built by ephemeral or small streams where they emerge from steep slopes onto flat plains or into swamps.

Pa — **Braided stream alluvium** (Late Pleistocene) - Fluvially deposited sand, silt, gravel and occasional muck on terraces (higher than Qst terraces) cut into glacial deposits in the Androscoggin River valley. In places, several succeedingly higher terraces are recognizable within this unit. These terraces formed during late-glacial time as sea level regressed. From 0.5 to 5 m (1 to 15 ft) thick.

Pmrs — **Marine regressive sand deposits** (Pleistocene) - Sand, silt, and minor gravel. Consists of reworked marine delta, outwash, and bottom materials redistributed by marine currents and wave action as sea level fell during late-glacial time. As much as 3 m (10 ft) thick.

Pgi — **Undifferentiated ice-contact deposits** (Pleistocene) - Sand, gravel, and silt. Consists of thin glaciofluvial outwash and/or ice-contact deposits. May include esker or glaciomarine fan deposits. Thickness varies from 0 to 6 m (0 to 20 ft).

Pmn — **Marine nearshore deposits** (Pleistocene) - Sand, gravel, and clay-silt deposited as a result of wave activity in nearshore or shallow marine environments. Includes some beach deposits. In places, coated with unmapped thin dune deposits. Thickness varies from 0.5 to 5 m (1 to 15 feet).

Pmdi — **Glaciomarine ice-contact delta deposits** (Pleistocene) - Composed primarily of sorted and stratified sand and gravel. Consists of ice-contact delta deposits graded to the contemporary sea. Distinguished by flat top (sometimes kettled) and foreset-topset beds. Thickness varies from 0.5 to 30 m (1 to 100 feet). Two deltas have been assigned the unique geographic names listed below:

Pmdigl - Gracelawn delta; topset-foreset contact at elevation 336 feet (102 m). (Thompson and others, 1989)
Pmdia - Armory delta

Pp — **Presumpscot Formation: Glaciomarine bottom deposits** (Pleistocene) - Silt and clay with local sandy beds and intercalations. Consists of late-glacial fine-grained (marine mud) bottom deposits. Commonly lies beneath surface deposits of units Pmdi, Pm, and Pmrs; in places, may be coated with unmapped thin dune deposits. As much as 50 m (150 ft) thick.

Pge — **Esker deposits** (Pleistocene) - Sand and gravel deposited by glacial meltwater flowing in tunnels within or beneath the ice. As much as 21 m (70 ft) thick.

Pt — **Till** (Pleistocene) - Light- to dark-gray, nonsorted to poorly sorted mixture of clay, silt, sand, pebbles, cobbles, and boulders; a predominantly sandy diamicton containing some gravel. Generally underlies most other deposits. Thickness varies and generally is less than 6 m (20 ft), but is probably more than 30 m (100 ft) under many drumlins and streamlined hills. Many streamlined hills in this area are bedrock-cored.

 — **Bedrock exposures** - Not all individual outcrops are shown on the map. Gray dots indicate individual outcrops; ruled pattern indicates areas of abundant exposures and areas where surficial deposits are generally less than 3 m (10 ft) thick. Mapped in part from aerial photography, soil surveys (McEwen, 1970), and previous geologic maps (Prescott, 1968).

Legend for Figure 4.1.4

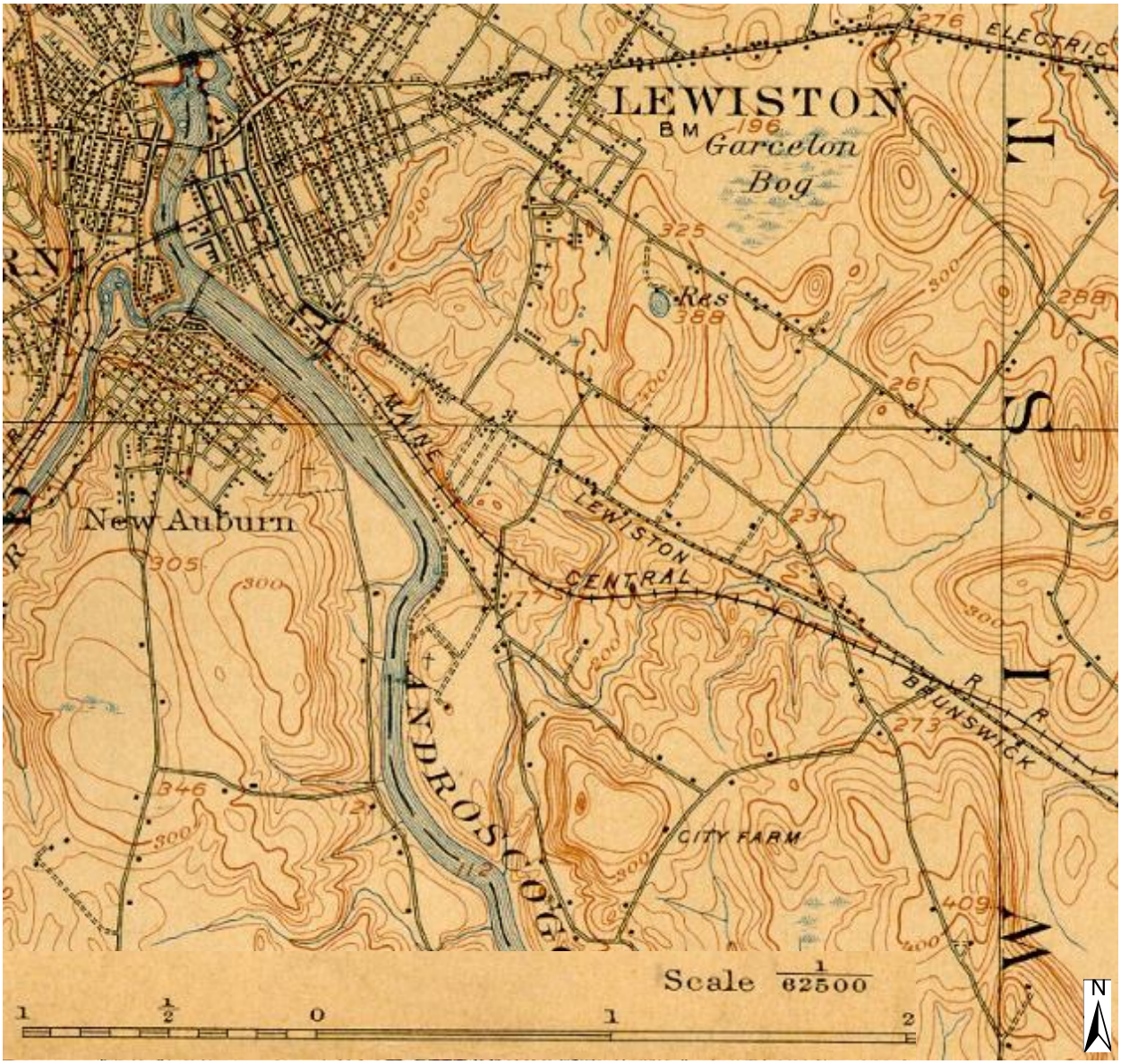

Figure 4.1.5: 1908 Historic map of Lewiston and the Hart Brook watershed (USGS)

Historical Sedimentation:

The historical sedimentation theory is somewhat of a hybrid between the Holocene and the Modern theories. It is based upon the raw lead data and the uppermost 60cm of reliable normalized lead data, but does not depend upon the radiocarbon date, and, in fact necessitates that the dated wood fragment was from a root. Therefore, this sedimentation theory is constrained by two lead events: the onset of the burning of leaded gasoline in 1923 (base of the lead concentration peak at 60cm see Fig 3.5.1) and the Clean Air Act outlawing the use of leaded gasoline in 1972 (the peak of lead concentrations at 40cm, see Fig 3.5.1). These events allow for two separate sedimentation rates to be calculated. Instead of an unconformity at 60cm (as in the Holocene theory), this theory assumes that sedimentation continued back in time at an average of the two modern rates. Changes in stratigraphy are more so a product of natural stream processes and development than any glacial or flooding events. The sedimentation rates and units are described below.

The rates were found to be 0.42 cm/yr from 1923 to 1972 and 0.85 cm/yr from 1972 to 2017, naturally the same values as the Holocene theory because both used the raw lead data. At this point, the Holocene and historical theories diverge from one another. In the Holocene theory, the sedimentation below 1923 was assumed to have been deposited by post-glacial marine transgression (approximately 10,000 years ago). Following marine sedimentation, there would have been a longstanding unconformity until impervious development generated enough energy from runoff to restart sedimentation (likely in the early 1900s at the soil clay boundary of 60-65cm). This theory does not assume that the clay and gravel layers below 65 cm are deposited by glacial processes, but instead are simply a further extension of modern sedimentation. To extrapolate back in time, the two known rates were averaged. The average rate, 0.64 cm/yr, was applied through the end of the 150cm core. In this theory 150cm represents the year 1781. The evidence in support of this theory is the raw lead data and the lack of a visible unconformity between the soil and clay layers.

The oldest sedimentological unit, the sand and gravels layers characterized by upward fining sequences, are likely the product of a migrating point bar in this theory. The historical model predicts that the sequences would repeat themselves approximately every 75 years. The overlaying clay unit may have formed by the pooling of water on the floodplain, in which the fine sediments had time to settle out. Another option would be that the fine sediments were reworked from upland areas and settled out when they reached the even elevation of the flood plain. The soil unit likely formed through the deposition of organic sediments from the upland sections of the watershed, a similar process in all three theories.

This sedimentation theory does not have an explicit argument to suggest a relationship between sedimentation and urbanization within the relative rates of sedimentation compared to rates of urbanization. It also does not suggest that depositional events were restarted or affected by an increase in runoff or the flowrate of runoff. An argument that can be made, though, for every theory is that modern sedimentation is happening at rate that far exceeds expected natural rates of sedimentation on floodplains. Referring back to a previous source (Pizzuto et al., 2016) that calculated the average rates of accumulation on 107 different floodplains, values ranged from 3.8 cm/100 years, 1.37 cm/100 years, 0.4 cm/100 years, 0.1 cm/100 years. The sedimentation values in every model of this study produce similar amount of sediment on an annual basis.

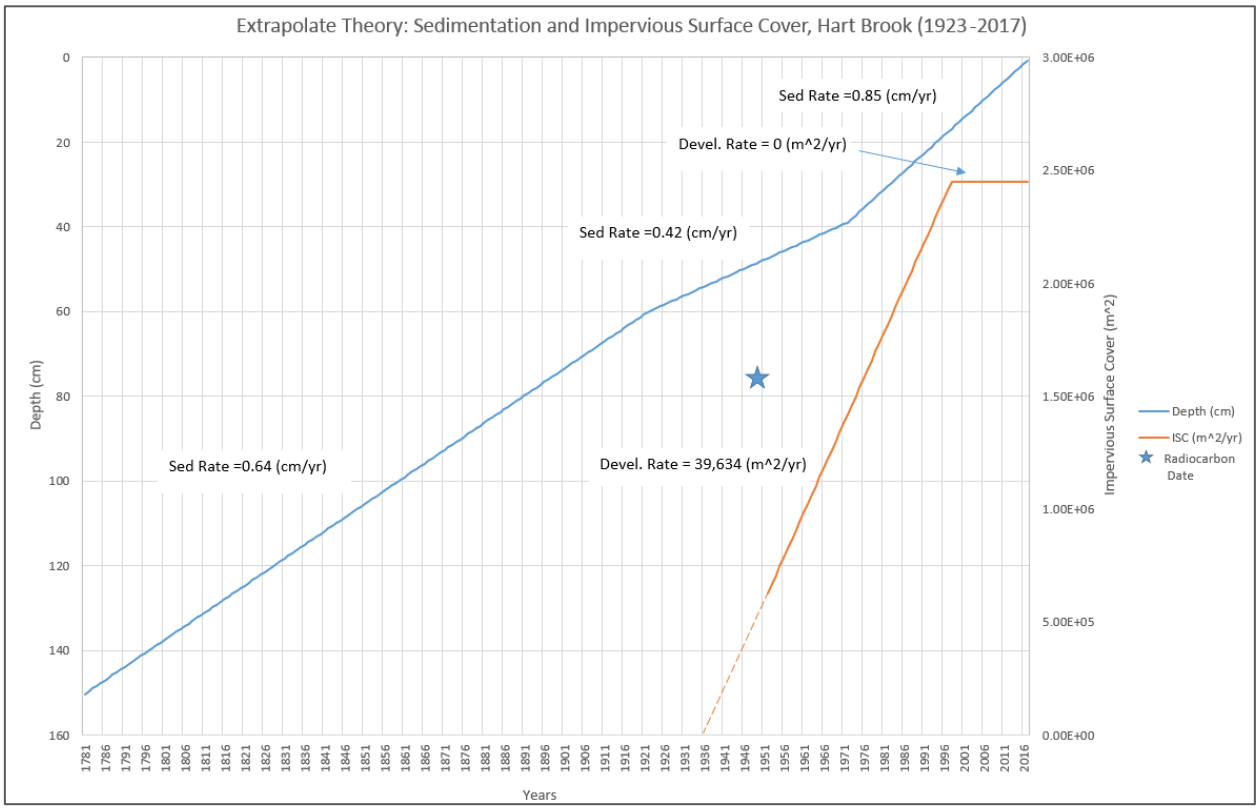

Figure 4.1.6: Historical Sedimentation Theory: Sedimentation and ISC from 1781-2018

To conclude, it becomes apparent that no matter the overall paleo-environmental setting, urbanization likely played a major role in recent sedimentary processes of the Hart Brook watershed. In the modern-core theory the most glaring evidence for the impact of development was the rapid rate and magnitude of sedimentation within the past-century, particularly between 1923 and 1972 at 2.4cm per year (fig 4.1.1). In the Holocene theory, it was the restarting of sedimentary processes after an extended unconformity. Finally, in all of the theories the sedimentation rate exceeds that of typical natural

floodplains. Outside influence of urbanization upon the natural hydrologic processes appears the only factor present to produce such a marked difference in rates, nearly two orders of magnitude. Further research is needed to bolster the relationship between the two variables (sedimentation and urbanization), such as town construction records or tax maps that could place additional constrains on development rates. Additional radiocarbon dating and coring could provide more knowledge related to sedimentation rates. Eventually, if enough data was available a regression could be run and would be a helpful analytical tool in quantifying the relationship between sedimentation and urbanization.

4.2 Spatial Analysis

As described in the methods section and displayed in the results of this paper, impervious surface calculations for the Hart Brook Watershed were performed in two separate ways and the methods of a previous calculation were unknown. It is important to compare the advantages and disadvantages of each method and to address why both of the calculations in this study yielded higher percentages than the previous estimate of percent impervious surface cover in the watershed.

The first method used data from the National Land Cover Dataset (NLCD). NLCD data is a sophisticated and open-access database of satellite and aerial imagery analysis for land cover classification. There are four primary datasets available (circa 1992, 2001, 2006, and 2011). This study used the most up-to-date 2011 dataset, which employs a Comprehensive Change Detection Model (CCDM). CCDM integrates two patented algorithms, a Multi-Index Integrated Change Analysis (MIICA) and Zone. The MIICA model uses spectral indices, which are essentially classifications of wavelength (pixel color), to track changes from one image to another (Jin et al., 2013). The Zone algorithm extracts change from two Landsat image pairs. Additionally, the 2011 dataset used a new technology to account for error typically caused by cloud cover and shadows. The technology can detect blue, shortwave infrared, and thermal infrared bands, rather than simple, spectral data. This allows the detector to recognize the difference between what is a cloud and what is something that is the color of a cloud on the Earth's surface. Finally, these areas are given clean pixel values and restored in a process called Spectral Similarity Grouping (SSG). SSG references a previous Landsat image to find an alternative similar pixel that could replace the pixel in question.

A second, tracing based method of impervious surface cover was selected as an alternative to the NLCD calculation because analysis of historical images was required and could not be achieved using the NLCD dataset (the earliest data is from 1992). The tracing method, as described in the methods section, was done using a modern aerial image basemap overlain by georeferenced historical aerial images in ArcGIS. The imagery was imported Landsat images, which were then transformed into polygon data and

clipped to the size of the watershed. A new, ISC polygon was then created by tracing the area of every visible developed section of the map. This step was repeated for the 1953 and modern images, individually. Finally, using the same development values and descriptions from the NLCD method each area was classified as a particular type of development, either medium intensity, high intensity, which had a specific %ISC value, 65% and 90%, respectively. This method, the tracing method, had far more opportunity for error than the previous NLCD method. First, it placed all trust in human dexterity rather than a mathematical algorithm. There is no way of ensuring that you can trace the boundaries of every pavement, neighborhood, etc. consistently. Additionally, land type ISC values were built and designed to fit the NLCD algorithm rather than any method of tracing, so there is a significant chance that the tracings will not fit perfectly into a particular category. Despite the somewhat more imprecise results of the tracing method, the values for the two permutations still fall directly between the 22% of the W&C estimate and 32.6% for the NLCD estimate, at 25.04% for all medium intensity development and 29.85% for half medium, half high intensity development. Likely, the second estimate is slightly more accurate as it accounts for not only an increase in the overall amount of developed area, but also an increase in the density of development between 1953 and 2017.

Methods were not reported for the original W&C 22% ISC estimate. That said, this study was able to access the original W&C GIS data and extrapolate the most likely tactics used. Fig. 4.3.1 shows a visual comparison between the NLCD and W&C methods. At first glance, the W&C method (right) may appear to be more sophisticated and detailed, but there are a few key methodological errors to address.

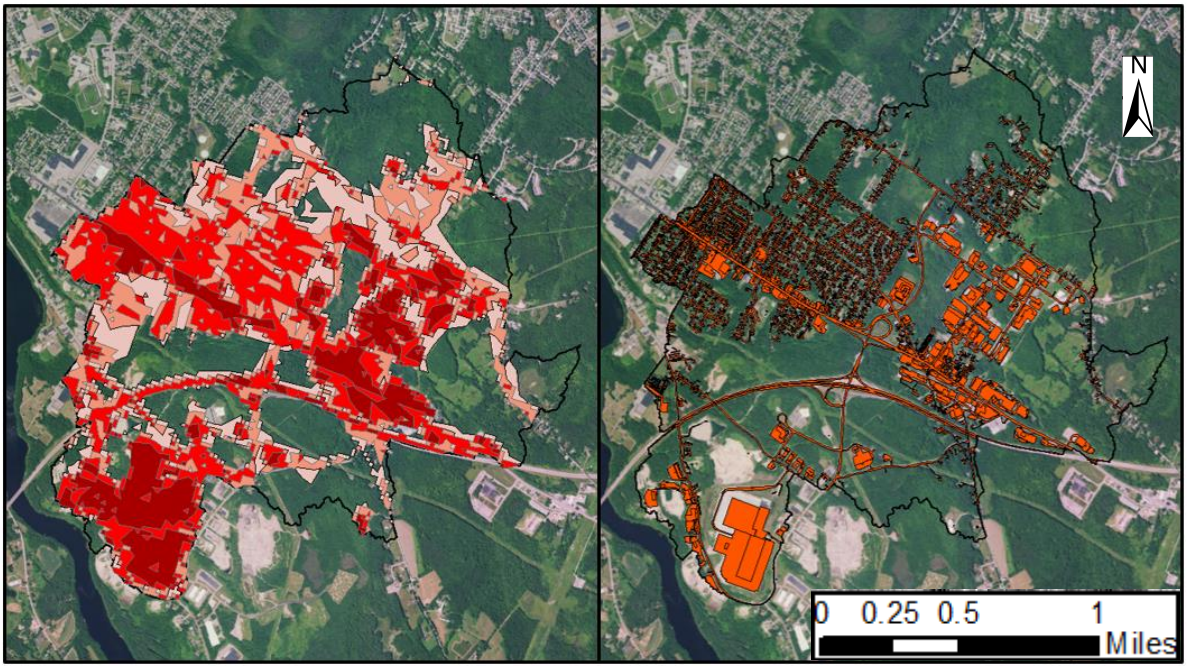

*Figure 4.2.1: (Left) NLCD Method *NOTE: not all areas highlighted are ISC. Highlighted areas correlate to a land type with a given range of % impervious cover see Fig 2.1.1 (Right) W&C tracing method*

The high level of infrastructural detail of the tracings of the roadways suggests that the W&C method may have used a polygon of existing roadways and made supplemental visual observations of rooftops; this method can underrepresent the true extent of a road or structure, as it does not account for any surrounding disturbance to roadsides, vegetation, and soils. A pixel or spectral based calculation (left) will avoid the inherent error of tracing an image or manually surveying a roadway, as it is simply an algorithm based on pixel color (wavelength) rather than the blueprints of a roadway. That said, the NLCD calculation may have more error in another realm: pixilation. The NLCD is a national dataset and does not allow for as much regional detail as in the W&C calculation. This NLCD method of remote sensing categorizes a range of pixel colors as a specific land type, but, it is not done by direct visual analysis, whereas the W&C method likely incorporated a higher degree of visual observations. The level of detail is also function of the different types of data used in the NLCD and W&C, raster and vector, respectively. Raster data is common for remote sensing techniques, but mandates a specific pixel size. In the case of the NLCD and most Landsat images 30 meter resolution is used. In a watershed that is only 8,933,060 m^2, that pixel size creates a moderate amount of error because it is unable to capture and account for the high level of detail and color change in such a small area. The ideal spatial analysis of this watershed would be a calculation that employs NLCD spectral analysis computed at a higher resolution than 30 m^2.

4.3 Water Quality

With evidence of both urbanization-induced sedimentation and of a history of sanitation issues within the Hart Brook, what is causing continued low-levels of dissolved oxygen? Could it be both? These questions will require additional future work and begin to reach outside the realm of this study, but the following brief review will address what is known and what remains unknown.

Dissolved oxygen levels have been tracked in great detail since the early 2000s, particularly by CES Inc. within the past five years. Dissolved oxygen data suggests that the most afflicted sites continue to be HB-2 and HB-4. If not a current direct input of wastewater, could the low D.O. be a residual symptom of the extreme pollution and poor sanitation that plagued the stream only a little over half a century ago? Perhaps, the pathogens are no longer present but the excess of nitrogenous and organically rich inputs have persisted or not yet been exhausted, driving dissolved oxygen levels below normal healthy levels. There is no historical water quality record accessible before the mid late 1990s for the Hart Brook, but it seems possible that dissolved oxygen levels may still be recovering from even lower levels during the era of raw sewage runoff, potentially even comparable to the lack of any dissolved oxygen in the Androscoggin River during the height of its pollution with sewage and paper pulp. Note this theory still holds significance to the concepts of urbanization and poor water quality. ISC can

accelerate the transportation of many pollutants that lay in the path of runoff into the stream, be it waste or sediments.

Lastly, if it is neither a current or historic input of waste, the only plausible variable remaining is excessive sedimentation and the addition of nitrogenous fertilizers through increased impervious surface runoff. This study provides the most concrete evidence in support of an increase in sedimentation along with increased urbanization, but the direct relationship to dissolved oxygen could be investigated further. Turbidity data and other sedimentary analyses are needed.

4.4 Global Implications

Within its recent history, the Hart Brook has faced many of the challenges, particularly water quality issues related to sanitation, that developing nations are facing today. Looking back to the introduction, in the late 1950s it was reported that sewage contamination, due to the lack of a formal sewer system, was causing public health issues in the Lewiston community. Not only was the smell unbearable, but there were reported cases of typhoid and staphylococcus. It was explicitly stated in the Lewiston Evening Journal in 1959 that the development boom throughout the 50s is what triggered the bacterial contamination of the Hart Brook. Global development is intimately connected to discussions of sedimentation rate, impervious surface cover, and public health. In the coming decades the areas that will experience the majority infrastructural expansion are also the areas with the least access to improved sanitation (WHO, 2014). The following portion of the discussion will describe the connections between development, potability, and sanitation with a heavy focus on the regions of the world at the highest risk of losing access, or never gaining access, to clean drinking water resources.

Access to Clean Drinking Water:

Globally, 1 out of 11 people lack access to safe drinking water, 783 million people (WHO, 2014). The vast majority of unclean drinking water is contaminated by bacteria from a lack of proper sanitation. The bacteria proliferates waterborne illnesses and diarrheal diseases, which account for 5.4 % of all deaths or 1.54 million deaths annually in developing countries (WHO, 2014). Along with HIV and perinatal conditions, bacterial diseases are arguably one of the most preventable health issues. Equally distressing, is that the most affected demographic is children below the age of five (WHO, 2014).

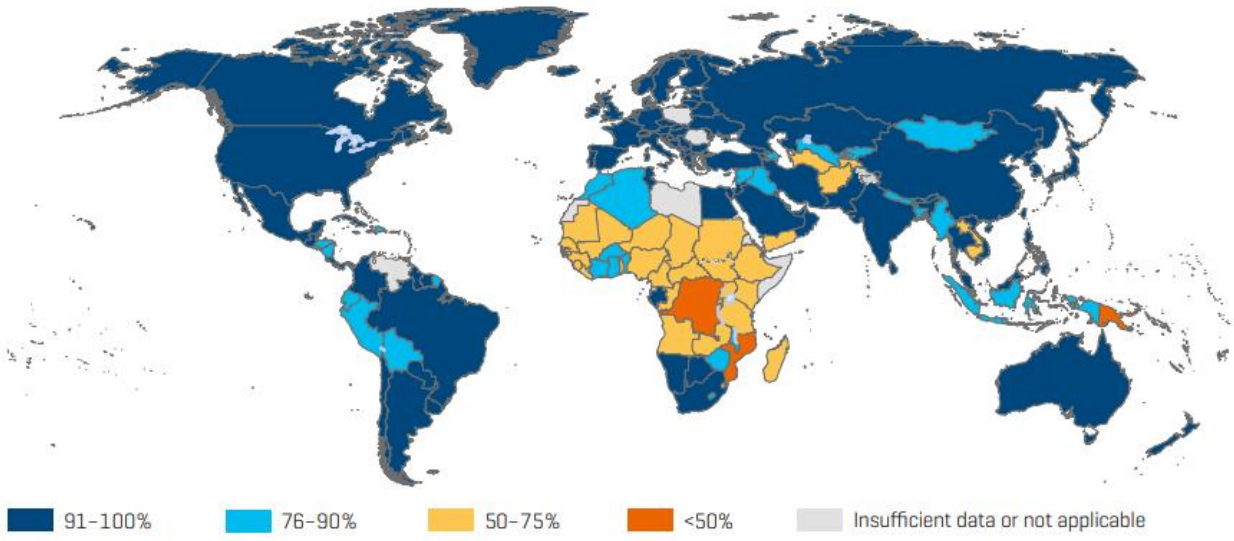

Figure 4.4.1: Global Drinking Water: Percent of national population with access to improved drinking water sources 2012 (WHO, 2014)

Sanitation:

Globally, approximately 2.5 billion people lack improved sanitation (see definition in WHO, 2014), and 1.1 billion people (15 per cent of the global population) practice open defecation (WHO, 2014). Standards of sanitation vary, but open defecation is arguably the most detrimental to drinking water resources, as it can be most easily transported into a water supply.

Strikingly, fig 4.5.1 and fig 4.5.2 show an immense amount of overlap in most affected regions, particularly Sub-Saharan Africa and countries in the South China Sea (Indonesia, Philippines, Papa New Guinea) (WHO, 2014). The overarching trend is clear; most regions without access to proper sanitation do not have access to clean drinking water. This seems intuitive, without sanitation bacteria are easily transported into local drinking water and cause illness to consumers. But a large question remains: What is the mechanism of transport? Could this problem be exacerbated by impervious surface development, one of the most efficient hydraulic pathways?

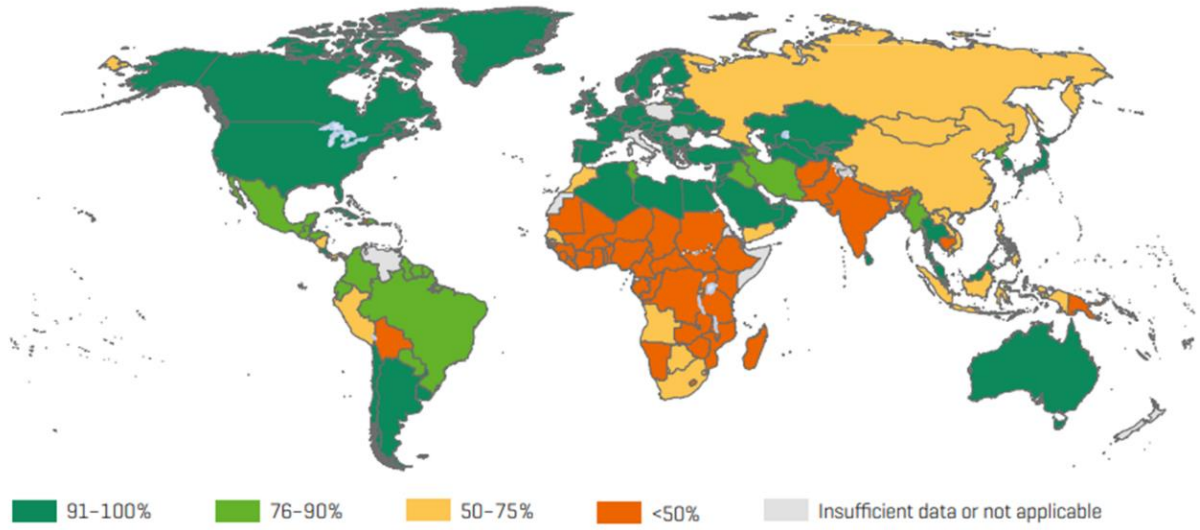

Figure 4.4.2: Global Sanitation: Percent of national population with access to improved sanitation in 2012 (WHO, 2014)

Development and Impervious Surface Cover:

If impervious surfaces are as good of a transport mechanism for bacteria as they are for sediments, than development trends show an ominous cloud on the horizon. Fig 4.5.3 shows that between 2000 and 2015, cities between 5 and 10 million residents and 10+ million residents added nearly 100 million new residents in developing regions (Cohen, 2006). Developed regions added only a small fraction of that figure, approximately 10 million new residents (Cohen, 2006). Additionally, smaller cities of less than 1 million residents added over 500 million new residents in developing countries and only approximately 30 million residents in developed countries, further highlighting the discrepancy of developing and developed urban expansion (Cohen, 2006).

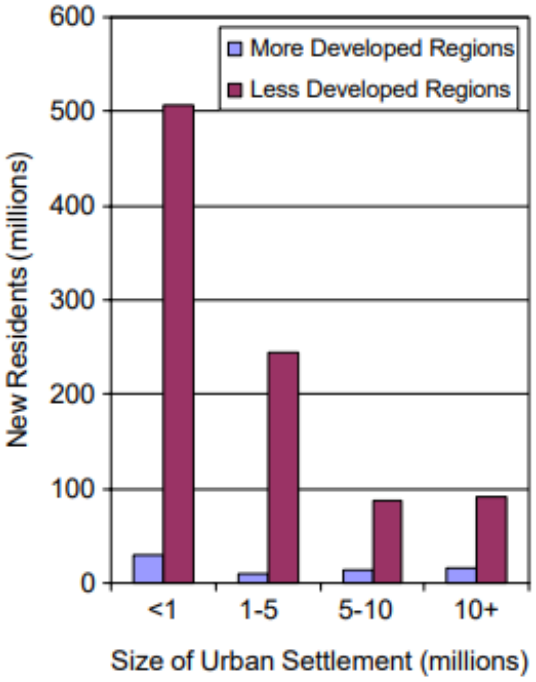

Figure 4.4.3: Urban Growth: the number of residents added to the urban areas between 2000 and 2015 based on the size of the urban settlement (in millions) (Cohen, 2006)

In addition to the magnitude of up and coming urban areas in developing countries, there is already a clear lack of sanitation and accessible drinking water, especially in Sub-Saharan Africa. Fig 4.4.4 shows that in cities of under 100,000 nearly 50% of people do not have access to piped water, flush toilets, and electricity (Cohen, 2006).

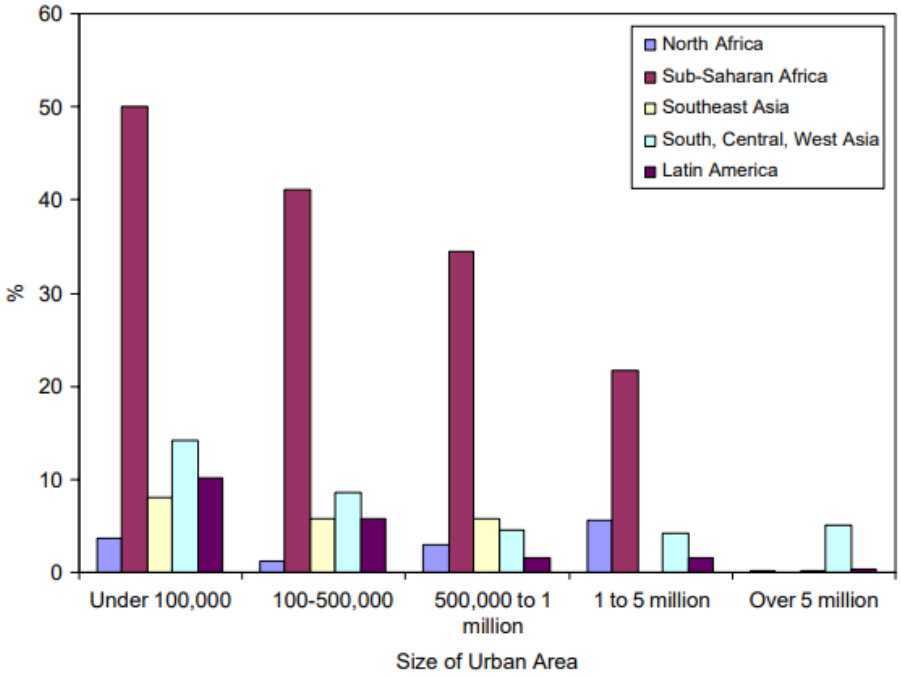

Figure 4.4.4: Urban Sanitation: percent of population without access to piped water, flush toilets, and electricity by the size of the urban area (Cohen, 2006)

The figures and text in this discussion of global development should be viewed as the identification of a potential development challenge that needs additional research and consideration. To date, there are very few sources that connect drinking water, sanitation, and development trends, especially in relation to the hydrologic transport of bacteria. The Hart Brook case study serves as an example of hydrologic regime changes that may occur when the general structure of a watershed is vastly altered in a relatively short period of time. Changes to sediment dynamics and baseflow or runoff behavior due to impervious surface cover have been cited by: Booth (1990), Brabec et al. (2002), Krug and Goddard (1986), Walters (2003), Ormerod (1998), Klein (1979) and Freeman and Shorr (2004). The trend of ISC alteration is clear, but the exact impacts on bacteria and waterborne disease are not, and must be studied.

5. Conclusions

The three theories of sedimentation found by using a combined age-dating model of lead concentrations and radiocarbon all provided evidence of rapid, modern sedimentation. Each sedimentation theory had strengths and drawbacks, but, in review, not all theories were equally compelling. This section will briefly address the strengths and weaknesses of each theory and propose that the historical sedimentation theory is the best model for the Hart Brook watershed.

The modern sedimentation theory was the only theory to incorporate the radiocarbon date and to claim that lead concentrations never returned to baseline values. This would necessitate that all 150cm of the HB-3 core were deposited since 1923. That magnitude of sedimentation on a floodplain would be nearly unprecedented within a floodplain environment. And, although it may appear that the normalized lead values never stabilize at a "baseline" concentration, the very small % carbon values at depths between 60 and 150 cm are below 1% and can exaggerate the amount of variability when in such small proportions. Additionally, the raw lead data shows, perhaps, the most well-defined trend that can be directly compared to other records and known changes in human activity.

The Holocene sedimentation theory is essentially the opposite end-member of the modern sedimentation theory. It represents time on a geologic scale and records activity related to glacial processes. The best evidence to challenge this theory is the lack of a well-defined unconformity or sharp boundary between the soil and clay layers. If this boundary truly represented the restarting of sedimentation after a long-standing unconformity, the soil would likely be deposited directly on top of a compact layer of clay without much integration or intermixing. Instead this boundary is gradational over more than five centimeters from 60-65 cm. This sedimentation rate in this theory is also the farthest offset from the 1950 radiocarbon date at 74cm.

The historical sedimentation theory incorporates the best element of the Holocene theory: the analysis of raw lead data in the upper 60 cm, including both the onset and peak of burning of leaded gasoline. By diverging thereafter from the Holocene theory and applying an average sedimentation rate (still high compared to other floodplains) to the bottom 60-150cm, some connections to urbanization may be lost. This theory does not propose an exorbitantly high sedimentation rate or the restarting of modern sedimentation, but with such a clear raw lead dataset and without an unconformity it is more likely that sedimentation patterns have shown some amount of consistency over time than incurred any radical transformation. It is still possible or even probable that sedimentation has responded to increasing urbanization, but that it is simply not visible in this dataset. The favored historical sedimentation model only had a total of three dated depths. Further work is needed, particularly radiocarbon dating, to further

constrain variability in sedimentation. That work would build a broader foundation to make connections to urbanization. More constraints could also be placed on rates of urbanization by investigating town records of construction, land sales, or tax maps. More comparison-based evidence from other watersheds is needed to determine the extent or degree of the impact of urbanization on the high rate of sedimentation. Additional sedimentation analyses could also include water sampling to test for total suspended solids TSS and total dissolved solids TDS. CES Inc has begun measuring for turbidity and many more research opportunities and analyses could be found in those datasets related to photosynthetic activity or phenology.

A larger, perhaps more meaningful, conclusion was unearthed during this research project relating to global urban development and water resources. Although the evidence of bacterial contamination from sewage in the Hart Brook was predominantly anecdotal, it is worth considering and comparing to development trends. It is also worth asking where our society and governmental institutions at large should place emphasis on water quality related issues. Is a small urban stream with low dissolved oxygen worth our funding and remediation efforts? Is the Hart Brook the type of ecosystem that we wish to preserve? Or are there more important global issues, like impending bacterial contamination of urban watersheds and drinking water? Perhaps, the answer is that we care about both issues and should devote more time and attention to what areas are expected to undergo urban expansion in the near future. These are questions of ethics, priorities, politics, and beyond, each of which was generated and demanded by the data and interpretations found within these pages. The largest and loftiest hope of this study, is that it may leap off the page and into the minds of curious, caring, intellectuals for further thought.

References

Arnold Jr, C. L., and Gibbons, C. J., 1996, Impervious surface coverage: the emergence of a key environmental indicator: Journal of the American planning Association, v. 62, no. 2, p. 243-258.

Booth, D. B., 1990, Stream-channel Incision Following drainage-basin Urbanization: JAWRA Journal of the American Water Resources Association, v. 26, no. 3, p. 407-417.

Booth, D. B., and Jackson, C. R., 1997, Urbanization of aquatic systems: degradation thresholds, stormwater detection, and the limits of mitigation: JAWRA Journal of the American Water Resources Association, v. 33, no. 5, p. 1077-1090.

Boutron, C. F., Candelone, J.-P., and Hong, S., 1995, Greenland snow and ice cores: unique archives of large-scale pollution of the troposphere of the Northern Hemisphere by lead and other heavy metals: Science of the total environment, v. 160, p. 233-241.

Brabec, E., Schulte, S., and Richards, P. L., 2002, Impervious surfaces and water quality: a review of current literature and its implications for watershed planning: CPL bibliography, v. 16, no. 4, p. 499-514.

Chase, E. Sherman. A Twenty-Year Study of Pollution of the Androscoggin River. 1960

Cohen, B., 2006, Urbanization in developing countries: Current trends, future projections, and key challenges for sustainability: Technology in society, v. 28, no. 1-2, p. 63-80.

Daley, M. L., Potter, J. D., and McDowell, W. H., 2009, Salinization of urbanizing New Hampshire streams and groundwater: effects of road salt and hydrologic variability: Journal of the North American Benthological Society, v. 28, no. 4, p. 929-940.

Dearing, J.A., 1999, Environmental Magnetic Susceptibility: Using the Bartington MS2 System: British Library, no. 7, p. 1-54

Diaz, R. J. and R. Rosenberg (2008). "Spreading dead zones and consequences for marine ecosystems." science 321(5891): 926-929.

Elvidge, C. D., Tuttle, B. T., Sutton, P. C., Baugh, K. E., Howard, A. T., Milesi, C., Bhaduri, B., and Nemani, R., 2007, Global distribution and density of constructed impervious surfaces: Sensors, v. 7, no. 9, p. 1962-1979.

Freeman, P. L., and Schorr, M. S., 2004, Influence of watershed urbanization on fine sediment and macroinvertebrate assemblage characteristics in Tennessee Ridge and Valley Streams: Journal of Freshwater Ecology, v. 19, no. 3, p. 353-362.

Hall, F.R., 1998, Introduction to Sediment Magnetism: Including Discussions on Magnetic Susceptibility

Hildreth, C.T., 2002, Surficial geology of the Lewiston 7.5-minute quadrangle, Androscoggin County, Maine, p. 1-6

Jin, S., Homer, C., Yang, L., Xian, G., Fry, J., Danielson, P., and Townsend, P. A., 2013a, Automated cloud and shadow detection and filling using two-date Landsat imagery in the USA: International Journal of Remote Sensing, v. 34, no. 5, p. 1540-1560

Jin, S., Yang, L., Danielson, P., Homer, C., Fry, J., and Xian, G., 2013, A comprehensive change detection method for updating the National Land Cover Database to circa 2011: Remote Sensing of Environment, v. 132, p. 159-175.

Karn, S. K., and Harada, H., 2002, Field survey on water supply, sanitation and associated health impacts in urban poor communities-a case from Mumbai City, India: Water Science and Technology, v. 46, no.11-12, p. 269-275.

Kaushal, S. S., Groffman, P. M., Likens, G. E., Belt, K. T., Stack, W. P., Kelly, V. R., Band, L. E., and Fisher, G. T., 2005, Increased salinization of fresh water in the northeastern United States: Proceedings of the National Academy of Sciences of the United States of America, v. 102, no. 38, p. 13517-13520.

Klein, R. D., 1979, Urbanization and stream quality impairment: JAWRA Journal of the American Water Resources Association, v. 15, no. 4, p. 948-963.

Krug, W. R., and Goddard, G. L., 1986, Effects of urbanization on streamflow, sediment loads, and channel morphology in Pheasant Branch basin near Middleton, Wisconsin: US Geological Survey.

Lawrance W.A. Androscoggin River Studies Seventeenth Annual Report, November, 1958, Series I: Androscoggin River 1940-1983, Subseries I: Androscoggin River Studies, Box 3, Folder 3, Walter A. Lawrance Papers, Edmund S. Muskie Archives and Special Collections Library, Bates College, Lewiston, Maine. (in press)

Lawrance W.A. Androscoggin River Studies Seventeenth Annual Report, November, 1959, Series I: Androscoggin River 1940-1983, Subseries I: Androscoggin River Studies, Box 3, Folder 3, Walter A. Lawrance Papers, Edmund S. Muskie Archives and Special Collections Library, Bates College, Lewiston, Maine. (in press)

MacDonald, A., and Davies, J., 2000, A brief review of groundwater for rural water supply in sub-Saharan Africa.

MDEP (2013). "TMDL Assessment Summary."

MDEP. (2013, 2014, 2015). Hart Brook (City of Lewiston). VRMP 2013 Data Report. Section 5-4.

Norton, S. A. (2007). Atmospheric metal pollutants-archives, methods, and history. Water, Air, & Soil Pollution: Focus **7**(1-3) p93-98.

Nriagu, J. O., 1990, The rise and fall of leaded gasoline: Science of the total environment, v. 92, p. 13-28.

NYC DEP. (2017). "Stormwater ".

Ormerod, L., 1998, Estimating sedimentation rates and sources in a partially urbanized catchment using caesium-137: Hydrological Processes, v. 12, no. 7, p. 1009-1020.

Owens, P. N., Walling, D. E., and Leeks, G. J., 1999, Use of floodplain sediment cores to investigate recent historical changes in overbank sedimentation rates and sediment sources in the catchment of the River Ouse, Yorkshire, UK: Catena, v. 36, no. 1, p. 21-47.

Pedersen, T. and S. Calvert (1990). "Anoxia vs. productivity: what controls the formation of organic-carbon-rich sediments and sedimentary Rocks?(1)." Aapg Bulletin 74(4): 454-466.

Pullan, R. L., Freeman, M. C., Gething, P. W., and Brooker, S. J., 2014, Geographical inequalities in use of improved drinking water supply and sanitation across sub-Saharan Africa: mapping and spatial analysis of cross-sectional survey data: PLoS medicine, v. 11, no. 4, p. e1001626.

Radtke, D., White, A., Davis, J., and Wilde, F., 1998, 6.2 Dissolved Oxygen: US Geological Survey TWRI, Book, v. 9, p. 26.

Renberg, I., Brännvall, M.-L., Bindler, R., and Emteryd, O., 2000, Atmospheric lead pollution history during four millennia (2000 BC to 2000 AD) in Sweden: AMBIO: A Journal of the Human Environment, v. 29, no. 3, p. 150-156.

Schueler, T. R., 1994, The importance of imperviousness: Watershed protection techniques, v. 1, no. 3, p. 100-111.

Shields, F. D., Lizotte, R. E., Knight, S. S., Cooper, C. M., and Wilcox, D., 2010, The stream channel incision syndrome and water quality: Ecological Engineering, v. 36, no. 1, p. 78-90.

Shotyk, W., Weiss, D., Appleby, P., Cheburkin, A., Frei, R., Gloor, M., Kramers, J. D., Reese, S., and Van Der Knaap, W., 1998, History of atmospheric lead deposition since 12,370 14C yr BP from a peat bog, Jura Mountains, Switzerland: Science, v. 281, no. 5383, p. 1635-1640.

Supply, W. U. J. W., and Programme, S. M., 2014, Progress on drinking water and sanitation: 2014 Update, World Health Organization.

W. B., and Borns, H. W., 1984, Surficial geologic map of Maine, Maine Geological Survey.

United Nations. (2014). "World Urbanization Prospects." Department of Social and Economic Affairs.

Walters, D., Leigh, D., and Bearden, A., 2003, Urbanization, sedimentation, and the homogenization of fish assemblages in the Etowah River Basin, USA, The Interactions between Sediments and Water, Springer, p. 5-10.

Weng, Q., 2012, Remote sensing of impervious surfaces in the urban areas: Requirements, methods, and trends: Remote Sensing of Environment, v. 117, p. 34-49.

Woodard (2007). Hart Brook Watershed Action Plan. Lewiston, ME.

Wu, R. S. (2002). "Hypoxia: from molecular responses to ecosystem responses." Marine pollution bulletin 45(1): 35-45.